Echocardiographic Assessment of the Canine Right Heart: Reference Intervals and Repeatability

Jessica M. Gentile

Thesis submitted to the faculty of the Virginia Polytechnic Institute and State University in partial fulfillment of the requirements for the degree of

Master of Science
In
Biomedical and Veterinary Sciences

Jonathan A. Abbott, Committee Chair
Martha M. Larson
David Panciera

January 27, 2012
Blacksburg, VA

Keywords: Echocardiography, Canine, Right heart, Reference Intervals, Repeatability

Echocardiographic Assessment of the Canine Right Heart:
Reference Intervals and Repeatability

Jessica M. Gentile

ABSTRACT

Objectives: *Phase 1)* Establish echocardiographic reference intervals for measurements of the normal canine right heart. *Phase 2)* Describe the repeatability of normal right heart echocardiographic measurements. *Phase 3)* Describe the repeatability of right heart echocardiographic measurements which predict pulmonary artery pressure.
Materials and Methods: *Phase 1)* 45 healthy adult dogs. Dogs underwent one echocardiographic examination by the same operator. *Phase 2)* 6 randomly selected dogs from the pool of Phase 1 dogs. Dogs underwent repeated echocardiograms by two operators. *Phase 3)* 4 client-owned dogs. Dogs underwent repeated echocardiographic examination by two operators.
Results: *Phase 1*) The linear relationship between dimension and transformed body weight was highly variable. For linear dimensions, most of the scaling exponents were close to the theoretical value of 1/3. For area measurements, most of the scaling exponents were close to 2/3. *Phase 2)* Of the 168 within-day, between-day and between-operator coefficients of variation (CV) generated, 154 (91.7%) were below 15% and 135 (80.4%) were less than 10%. *Phase 3)* Of the 100 within-day, between-day and between-operator CVs generated, 72 (72%) were below 20% and 46 (46%) were below 10%.
Conclusions: The right heart can be measured with relatively low repeatability. Measurement of the tricuspid regurgitation velocity should be the first priority when attempting to predict pulmonary artery pressure. If tricuspid regurgitation is not present, the use of transpulmonic acceleration time (AT) and the ratio of transpulmonic acceleration-to-ejection time (AT:ET) to indirectly assess pulmonary artery pressure is recommended.

Table of contents

List of Figures

Manuscript 1:

Manuscript 2:

List of Tables

Manuscript 1:

Manuscript 2:

List of Abbreviations

ARVC: Arrhythmogenic right ventricular cardiomyopathy
ASD: Atrial septal defect
ASE: American Society of Echocardiography
AT: Acceleration time
AT:ET: Ratio of acceleration time to ejection time
AT_ET_ratio_ L: Acceleration-to-ejection time ratio, measured from the left parasternal short axis
AT_ET_ratio_R: Acceleration-to-ejection time ratio, measured from the right parasternal short axis
AV: Aortic valve diameter
AV_L_sax_M: Aortic valve diameter, M-mode measurement from the left parasternal short axis
AV_R_sax: Aortic valve diameter, measured from the right parasternal short axis
BW: Body weight
CdVC: caudal vena cava diameter
CdVC_L4ch: Caudal vena cava diameter, measured from the left parasternal four-chamber
Co R: Repeatability coefficient
CT: Computed tomography
cTnI: Cardiac troponin I
CV: Coefficient of variation
DCRV: Double-chambered right ventricle
ECG: Electrocardiogram
endPI_PG_ L: Peak pressure gradient of end-diastolic pulmonic insufficiency, measured from the left parasternal short axis
endPI_PG_R: Peak pressure gradient of end-diastolic pulmonic insufficiency, measured from the right parasternal short axis
endPI_Vmax_ L: Velocity of end-diastolic pulmonic insufficiency, measured from the left parasternal short axis
endPI_Vmax_R: Velocity of end-diastolic pulmonic insufficiency, measured from the right parasternal short axis
ET: Ejection time
FAC_L4ch: Right ventricular fractional area change, measured from the left parasternal four-chamber
FS_R_lax: Fractional shortening, measured from the right parasternal long axis
FS_R_sax_M: Fractional shortening, M-mode measurement from the right parasternal short axis
IACUC: Institutional Animal Care and Use Committee
ISACHC: International Small Animal Cardiac Health Counsel
IVSd_R_lax: Interventricular septum in diastole, measured from the right parasternal long axis
IVSd_R_sax_M: Interventricular septum in diastole, M-mode measurement from the right parasternal short axis
IVSs_R_lax: Interventricular septum in systole, measured from the right parasternal long axis
IVSs_R_sax_M: Interventricular septum in systole, M-mode measurement from the right parasternal short axis
LBBB: Left bundle branch block
MPA: Main pulmonary artery diameter
MPA_L_sax: Main pulmonary artery diameter, measured from the left parasternal short axis
MR: Mitral regurgitation
MRI: Magnetic resonance imaging
PA: Pulmonary artery
PDA: Patent ductus arteriosus
PH: Pulmonary hypertension
PI: Pulmonic insufficiency
PI_maxPG_ L: Peak pressure gradient of pulmonic valve insufficiency, measured from the left parasternal short axis
PI_maxPG_R: Peak pressure gradient of pulmonic valve insufficiency, measured from the right parasternal short axis

PI_Vmax_ L: Peak velocity of pulmonic valve insufficiency, measured from the left parasternal short axis
PI_Vmax_R: Peak velocity of pulmonic valve insufficiency, measured from the right parasternal short axis
PS: Pulmonic stenosis
PTE: Pulmonary thromboembolism
PV: Pulmonic valve diameter
PV:AV: Ratio of pulmonic valve diameter to aortic valve diameter
PV_AT_ L: Trans-pulmonic acceleration time, measured from the left parasternal short axis
PV_AT_R: Trans-pulmonic acceleration time, measured from the right parasternal short axis
PV_AV_ratio_R_sax: Pulmonic valve to Aortic valve ratio, measured from the right parasternal short axis
PV_ET_ L: Trans-pulmonic ejection time, measured from the left parasternal short axis
PV_ET_R: Trans-pulmonic ejection time, measured from the right parasternal short axis
PV_L_sax: Pulmonic valve diameter, measured from the left parasternal short axis
PV_maxPG_ L: Peak pressure gradient of right ventricular ejection, measured from the left parasternal short axis
PV_maxPG_R: Peak pressure gradient of right ventricular ejection, measured from the right parasternal short axis
PV_R_sax: Pulmonic valve diameter, measured from the right parasternal short axis
PV_Vmax_L: Peak velocity of right ventricular ejection, measured from the left parasternal short axis
PV_Vmax_R: Peak velocity of right ventricular ejection , measured from the right parasternal short axis
RA Area: Right atrial area
RA Major: Right atrial major dimension
RA Major_L4ch: Right atrial major dimension, measured from the left parasternal four-chamber
RA Major_R_lax: Right atrial major dimension, measured from the right parasternal long axis
RA Minor: Right atrial minor dimension
RA Minor_L4ch: Right atrial minor dimension, measured from the left parasternal four-chamber
RA Minor_R_lax: Right atrial minor dimension, measured from the right parasternal long axis
RA_area_L4ch: Right atrial area, measured from the left parasternal four-chamber
RA_area_R_lax: Right atrial area, measured from the right parasternal long axis
RV FAC: Right ventricular fractional area change
RVd Area: Right ventricular area in diastole
RVd Major: Right ventricular major dimension in diastole
RVd Minor: Right ventricular minor dimension in diastole
RVd_area_L4ch: Right ventricular area in diastole, measured from the left parasternal four-chamber
RVd_Major_L4ch: Right ventricular major dimension in diastole, measured from the left parasternal four-chamber
RVd_Minor_L4ch: Right ventricular minor dimension in diastole, measured from the left parasternal four-chamber
RVFWd: Right ventricular free wall thickness in diastole
RVFWd_L4ch: Right ventricular free wall in diastole, measured from the left parasternal four-chamber
RVFWd_R_lax: Right ventricular free wall in diastole, measured from the right parasternal long axis
RVFWd_R_sax_M: Right ventricular free wall in diastole, M-mode measurement from the right parasternal short axis
RVFWs: Right ventricular free wall thickness in systole
RVFWs_L4ch: Right ventricular free wall in systole, measured from the left parasternal four-chamber
RVFWs_R_lax: Right ventricular free wall in systole, measured from the right parasternal long axis
RVFWs_R_sax_M: Right ventricular free wall in systole, M-mode measurement from the right parasternal short axis
RVIDd_R_lax: Right ventricular internal dimension in diastole, measured from the right parasternal long axis
RVIDd_R_sax_M: Right ventricular internal dimension in diastole, M-mode measurement from the right parasternal short axis
RVIDs_R_lax: Right ventricular internal dimension in systole, measured from the right parasternal long axis
RVIDs_R_sax_M: Right ventricular internal dimension in systole, M-mode measurement from the right parasternal short axis
RVOT: Right ventricular outflow tract diameter

RVOT:AV: Ratio of the right ventricular outflow tract diameter to aortic valve diameter
RVOT_AV_ratio_L_sax_M: Right ventricular outflow tract dimension to aortic valve diameter ratio, M-mode measurement from the left parasternal short axis
RVOT_L_sax: Right ventricular outflow tract, measured from the left parasternal short axis
RVOT_L_sax_M: Right ventricular outflow tract dimension, M-mode measurement from the left parasternal short axis
RVs Area: Right ventricular area in systole
RVs Major: Right ventricular major dimension in systole
RVs Minor: Right ventricular minor dimension in systole
RVs_area_L4ch: Right ventricular area in systole, measured from the left parasternal four-chamber
RVs_Major_L4ch: Right ventricular major dimension in systole, measured from the left parasternal four-chamber
RVs_Minor_L4ch: Right ventricular minor dimension in systole, measured from the left parasternal four-chamber
TAPSE: Tricuspid annular plane systolic excursion
TAPSE_L4ch_M: Tricuspid annular plane systolic excursion, M-mode measurement from the left parasternal four-chamber
ToF: Tetralogy of Fallot
TR: Tricuspid regurgitation
TR_maxPG_L: Peak pressure gradient of tricuspid regurgitation, measured from the left parasternal four-chamber
TR_Vmax_L: Peak velocity of tricuspid regurgitation, measured from the left parasternal four-chamber
TVAd: Tricuspid valve annulus in diastole
TVAd_L4ch: Tricuspid valve annular dimension in diastole, measured from the left parasternal four-chamber
TVAs: Tricuspid valve annulus in systole
TVAs_L4ch: Tricuspid valve annular dimension in systole, measured from the left parasternal four-chamber
TVD: Tricuspid valve dysplasia
VPC: Ventricular premature complex
VSD: Ventricular septal defect
WHWT: West Highland White Terrier

Introduction

Echocardiography is the use of medical ultrasound in cardiac imaging; it provides information that relates to cardiac structure, function and blood flow velocity. Because echocardiography is widely available and non-invasive, it is well-suited to both cardiac diagnosis and to serial assessment of patients with established cardiac disease. Historically, echocardiographic evaluation of left heart function has been emphasized but there has been recent interest in diseases characterized by changes in right ventricular structure and function including pulmonary hypertension (PH) and arrhythmogenic right ventricular cardiomyopathy (ARVC). Both of these disorders are important causes of morbidity and mortality in the dog; the latter is common in boxer dogs in which ARVC provides a model for human disease. Despite the importance of echocardiography in the evaluation of right heart disease, neither reference intervals for canine right heart dimensions, nor repeatability of echocardiographic indices of right heart structure and function have been reported.

Literature Review

The canine right heart is affected by many diseases, yet its echocardiographic evaluation has been incompletely standardized. This review will address congenital and acquired diseases that affect the canine right heart as well as diagnostic methods by which the right heart has been evaluated. Finally, we will summarize the development of echocardiographic reference intervals, including the use of allometric scaling and the importance of measures of repeatability.

Congenital diseases of the right heart

Pulmonic stenosis

In 1981, Patterson[1] et al described a heritable form of valvular pulmonic stenosis (PS) that occurred in a colony of Beagle dogs. All affected dogs had some degree of valvular thickening and these valves also had features of valvular hypoplasia or leaflet fusion. Patterson categorized the gross lesions: Grade 1 valves were minimally thickened and created minimal obstruction while grade 2 valves were moderately thickened with leaflet fusion, hypoplasia or both and created a moderate or severe obstruction. Three of 70 dogs also had other congenital defects: one had a patent ductus arteriosus, one had a ventricular septal defect and the other had both atrial and ventricular septal defects. Histologically, these dysplastic valves were characterized by thickening of the spongiosa layer with an increase in collagen and blood-filled spaces. Based on breeding experiments, Patterson characterized valvular pulmonic stenosis as a polygenic threshold trait.

In 1990, Buchanan[2] described the coronary artery anomaly called "R2A", in three bulldogs and a boxer dog with pulmonic stenosis. This anomaly is characterized by the presence of single coronary ostium, the right, which serves as the entrance to the right coronary artery from which arises a circumpulmonary left main coronary artery. In these four cases, the pulmonic stenosis was attributed to external compression of the right ventricular outflow tract by the anomalous course of the left main coronary artery. This report was supported by the experience of Kittleson et al[3]. They described two dogs that did not survive balloon valvuloplasty for pulmonic stenosis and were found to have the R2A anomaly on postmortem examination. Further investigation of this anomaly in English Bulldogs suggested that it is caused by a "malformation of the left aortic sinus of Valsalva and inversion of the proximal segment of the left main coronary artery."[4]

A number of invasive and minimally-invasive techniques have been developed to correct pulmonic stenosis. The first successful surgery for pulmonic stenosis utilized the open patch-graft technique without bypass or inflow occlusion.[5] A successful modified open technique was reported[6] and an open patch-graft using bypass was described for dogs less than 10 kilograms[7]. Other invasive techniques have also been described, including an arteriotomy using bypass in a beating heart for correction of supravalvar pulmonic stenosis[8] and the Brock procedure, involving transventricular pulmonic dilation.[9] Alternatively, a non-invasive procedure called balloon valvuloplasty was first described in a dog by Bright in 1997[10]. Further investigation into balloon valvuloplasty revealed that the optimum balloon-to-annulus ratio was 1.2-1.5 in uncomplicated cases[11]. In bulldogs with the R2A coronary anomaly, a balloon-to-annulus ratio of 0.6-1.0 is apparently safe and possibly effective[12]. While the balloon valvuloplasty procedure is

associated with some degree of myocellular damage[13], performed successfully it results in a 53% reduction in the risk of dying from heart failure sudden death or euthanasia because of heart failure[14]. In one study, the successful completion of a balloon valvuloplasty procedure was dependent on the conformation of the valve: almost all dogs with normal valve annuli survived the procedure and remained asymptomatic afterwards, while only two-thirds of dogs with hypoplastic valve annuli survived the procedure and only half of those remained asymptomatic afterwards[15].

Double-chambered right ventricle

The occurrence of double-chambered right ventricle (DCRV) in dogs was first described by Willard and Eyster[16] and then again by Koie[17]. Surgical correction under cardiopulmonary bypass in 7 dogs with DCRV has been reported; six dogs survived the immediate post-operative period and 4 survived long-term[18]. Another report of a dog with double-chambered right ventricle and tricuspid valve dysplasia included successful surgical correction of the DCRV using cardiopulmonary bypass.[19]

Tricuspid valve dysplasia/Ebstein's anomaly

Liu and Tilley[20] published the first veterinary case series of tricuspid valve dysplasia (TVD). Later, two retrospective investigations of canine congenital heart disease, determined that tricuspid valve dysplasia accounted for approximately 7.5% of the defects.[21, 22] Another study[23] found that the occurrence of tricuspid valve dysplasia or Ebstein's anomaly is 35 times greater in Labrador retrievers and 7 times greater in Boxer dogs compared to the general hospital population. Among Labradors, approximately

10% are affected[24] by tricuspid valve dysplasia, which is attributed to an autosomal dominant mutation on chromosome 9[25].

The primary gross pathologic findings of the first reported cases[20] included thickening of the tricuspid valve leaflets, abnormal development of chordae tendineae, papillary muscle hypertrophy, abnormal attachments of the leaflets to the ventricular walls and incomplete development of valve tissue. None of these patients had apical displacement of the valve tissue consistent with the malformation that occurs in human beings known as Ebstein's anomaly. Other concurrent congenital defects were common, including mitral valve dysplasia, ventricular septal defects, pulmonic stenosis, aortic stenosis and persistent left cranial vena cava. Electrocardiograms of these animals often revealed a rightward axis deviation and three had atrial fibrillation. DeMadron[26] also published a case report of a dog with tricuspid valve dysplasia and persistent supraventricular tachycardia and atrial flutter. Additionally, a splintered QRS occurs in 47% of Labradors, 60% of non-Labradors, and 67% of cats with tricuspid valve dysplasia[27]. Prior to the widespread use of echocardiography Eyster[28] reported the occurrence of Ebstein's anomaly in three dogs in which the diagnosis was confirmed by cardiac catheterization. Surgical intervention – one dog had tricuspid valve replacement and annular repair and one dog had atrial septal defect repair – was attempted unsuccessfully in two of Eyster's three cases[28]. In cases of tricuspid dysplasia in which the valve exhibits stenosis, a right atrial-to-pulmonary artery conduit (Fontan procedure)[29] and balloon valvuloplasty[30,31] have been described. Additional cases of canine Ebstein's anomaly have been reported[32, 33] which did not undergo surgical or catheterized intervention and were treated for congestive heart failure.

Atrial septal defect

A number of publications describe case series of dogs with atrial septal defects (ASD)[21,34-35]. Of the different ASD types, the ostium secundum is the most common, representing 98.7% of all ASDs in one study[36]. In these studies, echocardiography was used to diagnose the atrial septal defect, but the use of magnetic resonance imaging (MRI) to image an ostium secundum ASD has also been reported[37]. ASD occlusion has been reported with good short-term and mid-term outcomes[38-40].

Ventricular septal defect

Ventricular septal defects (VSD) can occur at any point in the interventricular septum and most often results in left-to-right shunting. VSDs have been reported to occasionally close spontaneously[41] which can result in the appearance of a septal aneurysm[42]. Closure of VSDs has been achieved by surgical correction under cardiopulmonary bypass[43,] minimally-invasive coil occlusion[44], and minimally-invasive VSD occluder placement[45,46]. The combination of systemic or suprasystemic pulmonary vascular resistance and a large VSD, referred to as Eisenmenger's syndrome, results in reversal of flow and a right-to-left shunting defect. This occurs rarely and has been reported once in a dog[47].

Tetralogy of Fallot

Patterson et al[48] described a spectrum of heritable conotruncal defects in Keeshond dogs that included tetralogy of Fallot (ToF). The defects were categorized as

follows: grade 1 consisted of minor structural abnormalities of the infundibulum, grade 2 consisted of grade 1 abnormalities plus pulmonic stenosis or a ventricular septal defect, and grade 3 consisted of grade 1 abnormalities, pulmonic stenosis and a ventricular septal defect. The genetics of Keeshond conotruncal defects have been explored[48-50], and eventually mapped to three canine chromosomes: CFA 2, 9 and 15[51]. Defects in at least two of these chromosomes are required for phenotypic manifestation of the conotruncal defects.

A number of interventions have been reported for palliation or repair of ToF. Use of the Blalock-Taussig shunt for palliation of ToF has been reported[52-53]; most dogs survived the immediate post-operative period and about half survived long-term. In addition, balloon dilation of the right ventricular outflow tract improved quality of life and short-term outcome in one dog[54]. Total open-heart repair of ToF has been reported using cardiopulmonary bypass with good intermediate- and long-term outcomes[55-56].

Patent ductus arteriosus

Analogous to a right-to-left shunting ventricular septal defect, a patent ductus arteriosus (PDA) in the presence of pulmonary hypertension due to increased pulmonary vascular resistance can result in a bidirectional or right-to-left shunt. This was first reported in a dog with polycythemia and seizures[57] and has been documented many times since[58-63]. Currently, the most common method of diagnosis is with echocardiography and a "bubble study", that is, the use of agitated saline to provide micro-bubble contrast[60,61,63], although the use of ^{99M}TC-microaggregated albumin has also been documented[64].

Surgical closure of left-to-right shunting PDAs with concurrent pulmonary hypertension has been performed successfully[65], but closure of right-to-left PDAs is not recommended. Long term management of a right-to-left shunting PDA using phlebotomy[66] and hydroxyurea[67] has been documented. Both methods improve polycythemia and the associated clinical signs.

Acquired diseases of the right heart

Arrhythmogenic right ventricular cardiomyopathy

The publication by Basso, et al, in 2004[68] established arrhythmogenic right ventricular cardiomyopathy (ARVC) in the Boxer Dog as an animal model of the human disease ARVC. Of the Boxer dogs examined, 39% experienced sudden death: three during exercise, four while walking slowly and two while sleeping. Another 13% were euthanized for refractory right-sided congestive heart failure. Syncope occurred in 52% of the dogs including two-thirds of the dogs that died suddenly.

Ventricular premature complexes (VPCs) with left bundle branch block (LBBB)-like morphology are the most common electrocardiographic finding and were documented in 83% of dogs in the Basso study[68]. Another 13% had VPCs of right bundle branch block-like morphology. In a separate study[69], normal adult Boxer Dogs that underwent ambulatory electrocardiograms had an average of 6 VPCs in a 24-hour period and most had fewer than 91 VPCs/24h. This may indicate an occult phase of ARVC but suggests that unequivocally affected Boxers have greater than 91 VPCs/24h. When Boxer Dogs with greater than 100 VPCs/24h were evaluated, the number of VPCs throughout the day was relatively consistent with a slight increase in occurrence between 8am – noon and 4pm – 8pm.[70]

On post-mortem examination[68], 35% of affected Boxer Dogs had gross right ventricular dilation and 13% had right ventricular aneurysms. All of the dogs examined had histological lesions: 65% had fatty replacement of the right ventricular myocardium and 35% had fibrofatty replacement. Nearly half of these dogs had left ventricular

infiltration as well, evenly split between fatty and fibrofatty tissue. In 35% the right or left atria also were histologically affected. Myocarditis of the right ventricle was seen in 65% of dogs, left ventricular myocarditis was present in 70% of dogs and 17% had left atrial myocarditis. Lending further support to the occurrence of myocarditis, Boxer Dogs with ARVC have elevated cardiac troponin I (cTnI) levels and their cTnI levels increase as the frequency of arrhythmias increase,[71] although this association could be complicated by arrhythmia-related ischemia.

Recently, Meurs, et al evaluated Boxer Dogs with greater than 500 VPCs/24h and identified a deletion mutation of the gene on chromosome 17 that encodes striatin.[72] Homozygous dogs were more severely affected based on number of VPCs recorded: homozygous median – 5,102 VPCs/24h, heterozygous median – 2,515 VPCs/24h, normal non-Boxer dog – 2 VPCs/24h. Inheritance is consistent with a co-dominant trait. Penetrance was 100% for homozygous dogs and 82% for heterozygous dogs. Striatin is a protein localized to the intercalated disc and contains a calcium-dependent site. At the intercalated disc, striatin interacts with the desmosomal proteins plakophilin-2, desmoplakin and plakoglobin. Mutation of genes that encode the latter three desmosomal proteins or desmoglein-2 were previously shown not to cause ARVC in Boxer Dogs.[73] Additionally, Boxer Dogs with ARVC have been shown to possess lower levels of myocardial calstabin-2, a protein which stabilizes the cardiac ryanodine receptor to prevent diastolic calcium leakage that could, in turn, cause ventricular tachyarrhythmias.[74]

In addition to extensive studies in Boxer Dogs, ARVC has also been documented in a Siberian Husky with ventricular tachycardia of LBBB-like morphology and a dilated

right ventricle[75], and in an English Bulldog with segmental right ventricular outflow tract ARVC[76].

Pulmonary hypertension

At the 4th World Symposium on Pulmonary Hypertension,[77] five clinical categories of pulmonary hypertension were proposed on the basis of pathophysiology, clinical presentation and therapeutic options. The first category encompasses pulmonary arterial hypertension, which can be idiopathic/inherited or associated with drugs/toxins, connective tissue disorders, HIV, portopulmonary hypertension, congenital heart diseases, schistosomiasis and chronic hemolytic anemia. The 1' category, a separate but associated category, comprises pulmonary veno-occlusive disease and pulmonary capillary hemangiomatosis. The second category includes pulmonary hypertension from left heart disease. The third category includes pulmonary hypertension from pulmonary diseases or hypoxia. The fourth category encompasses thromboembolic diseases. Finally, the fifth category encompasses cases that have unclear or multifactorial causes such as myeloproliferative disorders, neoplastic obstruction of airways, and metabolic disorders.

Category 1: Idiopathic/inherited PH

Case reports and small case series have described idiopathic arteriopathies in dogs. In one Pembroke Welsh Corgi[78], plexogenic pulmonary arteriopathy was diagnosed. The dog had pulmonary hypertension and a small patent ductus arteriosus of unknown significance. Post mortem examination revealed plexiform lesions of arteries

and small arterioles, intimal cellular proliferation and fibrosis, medial hypertrophy, fibrinoid degeneration and arteritis. Some small arteries were obliterated and there was hepatic congestion. A case series[79] described six dogs with pulmonary arteriopathies and severe PH. Four were female; four were intact. Four had medial hypertrophy, intimal thickening and concurrent plexiform lesions; one had isolated medial hypertrophy and one had medial hypertrophy with intimal thickening. One had isolated arteritis. Russell et al also described a dog with respiratory distress and severe PH[80]. The post mortem examination revealed acute necrotizing arteritis. Intimal and medial thickening and vascular obliteration was described by Glaus, et al, in a dog with PH and respiratory distress[81].

Category 2: PH from left heart disease

Serres et al documented PH in all stages of degenerative mitral valve disease, but prevalence of PH was associated with functional class: 3% in International Small Animal Cardiac Health Council (ISACHC) class Ia, 16.9% in class Ib, 26.7% in class II and 72.2% in class III[82]. In addition, this study noted a strong correlation between left atrial size and PH. Chiavegato et al also observed a positive association between estimated pulmonary artery (PA) pressure and indexes of left atrial size and left ventricular volume in dogs with PH and degenerative mitral valve disease[83].

Category 3: PH from diffuse pulmonary disease or hypoxia

Idiopathic pulmonary fibrosis is a condition that affects primarily terrier breeds, particularly the West Highland White Terrier (WHWT)[84]. Clinically, these dogs have

slowly progressive disease and experience cough, tachypnea, dyspnea, and exercise intolerance. Diffuse inspiratory crackles are the most common physical examination finding[85]. Blood gas analysis typically reveals hypoxemia secondary to a ventilation-perfusion mismatch[84,85]. Pulmonary hypertension is documented in approximately 52% of cases[84]. Histologically, the lungs of affected WHWTs contain locally extensive areas of alveolar septal fibrosis[84-86] , mineralization[86] and type-II pneumocyte hyperplasia[85,87]. Immunostaining reveals that the fibrosis is made up of predominently type III collagen with some type I collagen as well[87].

Category 4: PH from thromboembolic disease

Venous thromboembolisms are typically categorized as inherited or acquired in human medicine, however inherited hypercoagulability syndromes have not been identified in small animals. Documented risk factors for pulmonary thromboembolism (PTE) in dogs include: metabolic abnormalities (corticosteroid administration, diabetes mellitus, hyperadrenocorticism, hypothyroidism); cardiac disease (dirofilariosis, endocarditis, myocardial disease); sepsis and disseminated intravascular coagulation; surgery, trauma and indwelling venous catheters; immune-mediated hemolytic anemia, protein-losing nephropathy, neoplasia and pancreatitis.[88]

Clinical signs of PTE include dyspnea, tachypnea, coughing, cyanosis, syncope, collapse and sudden death. Upon physical examination, lung sounds may be harsh or muffled and a split S2 heart sound may be noted.[88] In addition to imaging studies such as pulmonary angiography, echocardiogram and computed tomography, blood tests like arterial blood gas A-a gradient, D-dimers, antithrombin activity and thromboelastography

may be useful in diagnosing hypercoagulable states and PTE.

Category 5: PH from unclear or multifactorial disease processes

The lungs of dogs severely infected by heartworms (Dirofiliaria immitus) reveal congestion, edema, hemorrhage, hemosiderin deposits, interstitial pneumonitis, thombi in small and large[89] arteries, fibrosis of the intima and media, and prominent post-obstruction anastamoses with bronchial arteries[90]. Additionally, dogs infected with heartworm have elevated endothelin-1, which contributes to vasoconstriction and cellular proliferation and may contribute to the development of PH[91]. Pulmonary hypertension has also been identified in dog infected with the European heartworm Angiostrongylus vasorum[92].

In one case report, diffuse bronchiolo-alveolar carcinoma in a dog resulted in respiratory distress, pulmonary hypertension and cor pulmonale[93].

Methods of evaluating the right heart

Thoracic Radiography

In general, thoracic radiographs may aid in the diagnosis of right heart enlargement, but rarely identify the cause. For example, radiographic right atrial enlargement may be seen in cases or tricuspid valve dysplasia or cor triatriatium dexter; right ventricular enlargement may be seen with pulmonary hypertension, pulmonic stenosis, tetralogy of Fallot, myxomatous tricuspid valve disease or dilated cardiomyopathy.[94] Lehmkuhl, et al, indexed the caudal vena caval diameter to the aorta, to the length of the thoracic vertebra above the carina and to the width of the right fourth ribs. Significant differences were found between the caval size of normal dogs and dogs with right heart disease, the majority of whom were in right-sided congestive heart failure. While diagnostic cut-offs were established, a clinically important amount of overlap exists between these groups[95]. Pulmonic stenosis may result in post-stenotic dilitation[94] of the main pulmonary artery. Pyle, et al, noted that dogs with right-to-left shunting PDAs had the following radiographic findings: small pulmonary vessels and a dilated descending aorta[58]. First-pass radionuclide angiocardiograms, which involve the injection of technetium-99m labeled boluses and scintigraphic imaging can be used to evaluate the right heart. In a study of dogs with mitral regurgitation, Carlsson, et al, used radionuclide angiocardiograms to show that the right heart was minimally affected by compensated mitral regurgitation (MR), but became dilated and compressed as the left heart enlarged[96]. They also noted that increased sternal contact was noted in all degrees of MR severity and was a poor indicator of right ventricular enlargement.

Electrocardiography

Similar to thoracic radiography, electrocardiography (ECG) is helpful for identifying right heart enlargement but generally not the underlying condition. One exception is the splintered QRS which is an insensitive but possibly specific electrocardiographic marker of tricuspid valve dysplasia. In one cohort, splintered QRS was identified in 47% of Labradors, 60% of non-Labradors, and 67% of cats with tricuspid valve dysplasia[27]. Another disease which may be presumptively diagnosed or at least, strongly suspected, based on electrocardiography is ARVC. As previously noted[69], normal adult Boxer dogs that underwent ambulatory electrocardiograms had an average of 6 VPCs in a 24-hour period and most had fewer than 91 VPCs/24h. This may indicate an occult phase of ARVC and also suggests that abnormal Boxers have greater than 91 VPCs/24h. Additionally, Spier, et al, used signal-averaged ECGs to show that the occurrence of late potentials in Boxer dogs with ARVC predicted the dogs that would experience sudden cardiac death or congestive heart failure[97].

Echocardiography

Echocardiography has been described as "an accurate, non-invasive method that can assess cardiac structure, function and blood flow dynamics".[98] In humans, echocardiography can be used to visualize the right heart, obtain dimensions[99] and functional indices of the right heart and to estimate pulmonary artery pressure[100]. In children, applying the modified Bernoulli equation to tricuspid regurgitation (TR) velocities measured by Doppler echocardiography is a valid estimate of pulmonary artery

pressure.[101] Among sick neonatal children, peak TR velocities were the most repeatable estimate of pulmonary artery pressure, compared to systolic time intervals (pulmonic valve acceleration time-to-ejection time (AT:ET) and pre-ejection period-to-ejection time) and PDA ductal flow[102]. Peak TR velocity and TR velocity at the time of valve opening have also been validated as estimates of systolic and diastolic pulmonary artery pressure in human adults[103,104]. Alternatively, in adults with PH from chronic pulmonary disease or thromboembolic disease, right ventricular ejection fraction measured by thermodilution is significantly correlated to tricuspid annular plane systolic excursion (TAPSE) and right ventricular fractional area change (FAC), both obtained with echocardiography[105]. Another study[106] found that diminished TAPSE is a highly specific marker of right ventricular systolic dysfunction, although this finding is less reliable in the presence of severe tricuspid regurgitation[107].

In dogs, the use of tricuspid regurgitation velocities to estimate pulmonary artery pressure has not been validated with respect to invasive pressure measurements, although it is often assumed to be valid based on the human studies. In a retrospective study of dogs with PH[108], peak TR velocities and peak pulmonic insufficiency (PI) velocities were used to identify systolic and diastolic PH respectively. This method of estimating pulmonary artery pressure has been the basis of multiple other studies. Serres, et al, documented an increase in prevalence of PH associated with greater functional impairment due to degenerative mitral valve disease and a correlation between an index of left atrial size and PH[82] was identified. Similarly, Chiavegato et al, observed a weak positive association between PA pressure and indexes of left atrial size and left ventricular volume in dogs with PH and degenerative mitral valve disease[83].

Systolic time intervals and other non-Doppler measurements have been examined in dogs with PH, as they have in humans. The use of systolic time intervals, which include the acceleration time (AT) of transpulmonic flow, the total ejection time (ET) of transpulmonic flow and the pre-ejection period of the right ventricle, and other measurements can be useful for identifying PH in patients without TR. For example, Schober et al examined healthy Boxer dogs, WHWT and WHWT with interstitial pulmonary disease (some with normal pulmonary artery pressures, some with PH and some with undetermined pulmonary artery pressure) using echocardiography. Focusing specifically on AT and AT:ET, normal values were established and cut-off values were determined that could identify the presence of PH[109]. These measurements were not affected by heart rate, body weight or right ventricular fractional shortening and were minimally affected by age. The repeatability of these measurements was not determined. These findings were supported by the work of Serres et al, who were able to show a significant correlation between pulmonary artery pressure and AT, AT:ET, the ratio of main pulmonary artery diameter to aortic diameter as well as the Tei index, which is a ratio of right ventricular isovolumetric contraction and relaxation time to ET[110].

Computed Tomography (CT)

Very little is written regarding cardiac CT in dogs; the majority of the literature is related to non-cardiac thoracic structures. In two studies, cardiac CT was performed on dogs that were used as models for human disease[111,112].

Magnetic Resonance Imaging (MRI)

The use of MRI to measure cardiac output[113] and cardiac mass[114] has been validated in dogs. MRI has also been used to provide three dimensional reconstruction and geometric characterization of the canine right ventricular free wall[115]. The widespread application of cardiac MRI is limited by the availability of ECG-gated MRI, thoracic wall motion, the need for anesthesia, and the need to develop refined technique protocols[116]. There have been some clinical applications, however. Using ECG-gated MRI, Baumwart et al showed that the right ventricular ejection fraction of Boxer dogs with ARVC is lower than that of healthy hound dogs; in that study, a right ventricular aneurysm was noted in one dog[117]. Cardiac MRI was used to evaluate the size of an ASD in a young German Shepherd dog with multiple congenital cardiac anomalies[118]. Finally a case series of ECG-gated MRI of two normal dogs and two dogs with heart base tumors contained a detailed description of a successful technique[119].

Allometric scaling

Allometry can be broadly defined as the description of the size of body parts as proportions of the whole. The allometric equation has the general form : $y = a M^b$, in which y is a measured dimension, M is body mass, a is known as the proportionality constant and b is the scaling exponent. Because mass is a surrogate measure of volume, measurements of length from geometrically similar objects have a linear relationship with the cube root of mass. Similarly, there is a linear relationship between measured areas and volumes to mass raised respectively to the exponents 0.67 and 1. The exponents in these theoretical relationships correspond to the scaling exponent of the allometric equation. The relationship between cardiac dimensions and body size have generally matched those predicted by allometric principles. Indeed, when Sisson and Schaeffer[120] examined the echocardiographic M-mode dimensions of the growing heart in dogs, they showed that heart size was not linearly associated with body weight. Instead, the size of the heart varied in association with body weight raised to exponents in the range of 0.31-0.45. Similarly Cornell, et al, showed that M-mode measurements of the canine heart did not have a linear relationship with body weight or body surface area[121]. Instead they found that most measurements had a linear relationship with body weight raised to an exponent that generally was close to 0.33, although end-diastolic left ventricular wall thickness had a linear relationship with body weight to the power of 0.25. They then used these findings to create prediction intervals for normal canine M-mode measurements. Hall, et al, performed a meta-analysis of numerous studies on canine

echocardiographic reference intervals and also used body weight to the 0.33 power to index measurements[122]. These measurements encompassed a wide range of body sizes and conformations. In addition, they showed that in growing dogs, the indexes stabilized around 12 weeks of age. Alternatively, Brown, et al, developed M-mode indexes using the aortic root diameter or the aortic root diameter indexed to body weight to the 0.33 power in dogs, cats and horses[123]. Justifications for allometric scaling comes not just from the veterinary literature[124], but from human literature, where allometric scaling has been used to predict echocardiographic measurements in adults[125] , children[126] and junior athletes[127], and also to define distinct prediction intervals for males and females[128]. Worth noting is that only one veterinary study utilized 2-D echocardiography[122] and only one study included a measurement of the right heart[120] (right ventricular internal diameter).

Repeatability

Repeated echocardiographic measurements obtained from healthy individuals are not identical but instead, vary because of operator and instrument factors as well as the inherent, biological variability in the quantity of interest. The description of measurement variation in healthy subjects, or in diseased, but clinically stable, patients, defines repeatability of the test and determines the magnitude of change that reflects a "real" or clinically relevant difference in measurements. Quantification of measurement variation is therefore essential for interpretation of echocardiograms serially obtained from patients with disease and this is the case if those echocardiograms are obtained from individual patients or in the context of clinical trials. The repeatability of selected

echocardiographic variables has been evaluated in healthy humans, dogs, cats, and horses.[99, 129-131] However, repeatability of 2D echocardiographic variables that describe the canine right heart has not been reported. Furthermore, measurement repeatability of TR velocity, the primary means by which PH is identified and monitored, has not been described in the dog. The evaluation of measurement variation in patients, rather than in healthy subjects, does raise questions regarding the stationarity of the data; quite obviously disease can get worse or, get better. However, it is accepted that repeatability can be assessed in patients with disease provided that the patients are clinically stable and studies are completed during a relatively short time-frame. There is precedent for this approach as repeatability of selected echocardiographic variables has been evaluated in dogs with tricuspid valve regurgitation[110] and people with other cardiac disorders including tricuspid valve regurgitation.[132-134]

Data Handling – Development of Reference Intervals

According to Jones and Barker, 2008[135], the recommended elements of a process for establishing a reference interval include:

• Define the analyte (measurement) for which the reference interval is being established, the clinical utility, biological variation and major variations in form.

• Define the method used, the accuracy base, and analytical specificity.

• Define important pre-analytical considerations together with any actions in response to the interference.

• Define the principle behind the reference interval (i.e. central 95% etc.)

• Describe the data source(s), including: number of subjects, nature of subjects, exclusions, pre-analytical factors, statistical measures, outliers excluded and analytical method.

• Define considerations of partitioning based on age, sex etc.

• Define the number of significant figures, i.e. the degree of rounding.

• Define the clinical relevance of the reference limits.

• Consider the use of common reference intervals.

• Decision and implementation.

This highlights the importance of clear definition of the measurement and narrow definition of the target population, in addition to the statistical calculation of the reference interval. [135].

Although the central 95% of observed measurements is sometimes used as an alternative, reference intervals are conventionally developed based on the observed mean and data dispersion. More specifically, the reference range typically consists of the interval bounded by 2, or 1.96, standard deviations above and below the observed mean. Optimally, the precision of point estimates – that is, confidence intervals about the mean and limits of the reference range - also are reported as in the recent American Society of Echocardiography (ASE) Guidelines for the Echocardiographic Assessment of the Right Heart in Adults[100]

Data Handling – Description of Variability

There exists some debate regarding the most appropriate way to assessed repeatability and reproducibility of measurements and the description of those

measurements variability. Bland and Altman[139] have advocated the use of standard deviation-based methods, from which a repeatability coefficient (Co R) can be calculated. By comparing the interval defined by – Co R and + Co R to the 95% limits of agreement, one can determine if differences in measurements differ because of a lack of repeatability or because of other factors that decrease agreement. This approach was utilized in Skinner, et al, 1996[101] to establish tricuspid regurgitation as the most repeatable echocardiographic estimate of pulmonary artery pressure in newborns.

In the veterinary literature, the vast majority of studies have utilized the coefficient of variation (CV), which describes the standard deviation as proportion of the mean and can be used to validate a measurement as "reliable". For example, the National Health Statistics report[140] flags values with CVs over 30% as "not meet[ing] standards of reliability or precision". CV has been used to describe variability or repeatability in the echocardiographic assessment of dogs, [122, 130, 136, 141-143] cats, [144-145] and horses.[137]

References

1. Patterson DF, Haskins ME, Schnarr WR. Hereditary dysplasia of the pulmonary valve in beagle dogs. Pathologic and genetic studies. Am J Cardiol. 1981 Mar; 47(3): 631-41.
2. Buchanan JW. Pulmonic stenosis caused by a single coronary artery in dogs: four cases (1965-1984). J Am Vet Med Assoc. 1990 Jan 1; 196(1): 115-20.
3. Kittleson M, Thomas W, Loyer C, Kienle R. Single coronary artery (type R2A). J Vet Intern Med. 1992 Jul-Aug; 6(4): 250-1.
4. Buchanan JW. Pathogenesis of single right coronary artery and pulmonic stenosis in English Bulldogs. J Vet Intern Med. 2001 Mar-Apr; 15(2): 101-4.
5. Breznock EM, Wood GL. A patch-graft technique for correction of pulmonic stenosis in dogs. J Am Vet Med Assoc. 1976 Nov 15; 169(10): 1090-4.
6. Hunt GB, Pearson MR, Bellenger CR, Malik R. Use of a modified open patch-graft technique and valvulectomy for correction of severe pulmonic stenosis in dogs: eight consecutive cases. Aust Vet J. 1993 Jul; 70(7): 244-8.
7. Tanaka R, Shimizu M, Hoshi K, Soda A, Saida Y, Takashima K, Yamane Y. Efficacy of open patch-grafting under cardiopulmonary bypass for pulmonic stenosis in small dogs. Aust Vet J. 2009 Mar; 87(3):88-93.
8. Soda A, Tanaka R, Saida Y, Yamane Y. Successful surgical correction of supravalvular pulmonary stenosis under beating heart using a cardiopulmonary bypass system in a dog. J Vet Med Sci. 2009 Feb; 71(2):203-6.
9. Saida Y, Tanaka R, Hayama T, Soda A, Yamane Y. Surgical correction of pulmonic stenosis using transventricular pulmonic dilation valvuloplasty (Brock) in a dog. J Vet Med Sci. 2007 Apr; 69(4): 437-9.
10. Bright JM, Jennings J, Toal R, Hood ME. Percutaneous balloon valvuloplasty for treatment of pulmonic stenosis in a dog. J Am Vet Med Assoc. 1987 Oct 15;191(8):995-6.
11. Estrada A, Moïse NS, Erb HN, McDonough SP, Renaud-Farrell S. Prospective evaluation of the balloon-to-annulus ratio for valvuloplasty in the treatment of pulmonic stenosis in the dog. J Vet Intern med. 2006 Jul-Aug; 20(4): 862-72.
12. Fonfara S, Martinez Periera Y, Swift S, Copeland H, Lopez-Alvarez J, Sumerfield N, Cripps P, Dukes-McEwan J. Balloon valvuloplasty for treatment of pulmonic stenosis in English Bulldogs with an aberrant coronary artery. J Vet Intern Med. 2010 Mar-Apr; 24(2): 354-9.
13. Saunders AB, Smith BE, Fosgate GT, Suchodolski JS, Steiner JM. Cardiac troponin I and C-reactive protein concentrations in dogs with severe pulmonic stenosis before and after balloon valvuloplasty. J Vet Cardiol. 2009 Jun; 11(1): 9-16.
14. Johnson MS, Martin M, Edwards, D, French A, Henley W. Pulmonic stenosis in dogs: balloon dilation improves clinical outcome. J Vet Intern Med. 2004 Sep-Oct; 18(5): 656-62.
15. Bussadori C, DeMadron E, Santilli RA, Borgarelli M. Balloon valvuloplasty in 30 dogs with pulmonic stenosis: effect of valve morphology and annular size on initial and 1-year outcome. J Vet Intern Med. 2001 Nov-Dec; 15(6): 553-8.
16. Willard MD, Eyster GE. Double-chambered right ventricle in two dogs. J Am Vet Med Assoc. 1981 Mar1; 187(5): 486-8.
17. Koie H, Kurotobi EN, Sakai T. Double-chambered right ventricle in a dog. J Vet Med

Sci. 200 Jun; 62(6): 651-3.
18. Martin JM, Orton EC, Boon JA, Mama KR, Gaynor JS, Bright JM. Surgical correction of double-chambered right ventricle in dogs. J Am Vet Med Assoc. 2002 Mar 15;220(6):770-4, 768.
19. Tanaka R, Shimizu M, Hirao H, Kobayaski M, Nagashima Y, Machida N, Yamane Y. Surgical management of a double-chambered right ventricle and chylothorax in a Labrador retriever. J Small Anim Pract. 2006 Jul; 47(7):405-8.
20. Liu SK, Tilley LP. Dysplasia of the tricuspid valve in the dog and cat. J Am Vet Med Assoc. 1976 Sept 15; 169(6): 623-30.
21. Tidholm A. Retrospective study of congenital heart defects in 151 dogs. J Small Anim Pract. 1997 Mar; 38(3): 94-8.
22. Baumgartner C, Glaus TM. Congenital cardiac diseases in dogs: a retrospective analysis. Schweiz Arch Tierheilkd. 2003 Nov; 145(11): 527-33, 535-6.
23. Chetboul V, Tran D, Carlos C, Tessier D, Pouchelon JL. Congenital malformations of the tricuspid valve in domestic carnivores: a retrospective study of 50 cases. Schweiz Arch Tierheilkd. 2004 Jun; 146(6):265-75.
24. Famula TR, Siemens LM, Davidson AP, Packard M. Evaluation of the genetic basis of tricuspid valve dysplasia in Labrador Retrievers. Am J Vet Res. 2002 Jun; 63(6): 816-20.
25. Andelfinger G, Wright KN, Lee HS, Siemens LM, Benson DW. Canine tricuspid valve malformation, a model of human Ebstein anomaly, maps to dog chromosome 9. J Med Genet. 2003 May; 40(5): 320-4.
26. de Madron E, Kadish A, Spear JF, Knight DH. Incessant atrial tachycardias in a dog with tricuspid dysplasia. Clinical management and electrophysiology. J Vet Intern Med. 1987 Oct-Dec; 1(4): 163-9.
27. Kornreich BG, Moïse NS. Right atrioventricular valve malformation in dogs and cats: an electrocardiographic survey with emphasis on splintered QRS complexes. J Vet Intern Med. 1997 Jul-Aug;11(4):226-30.
28. Eyster GE, Anderson L, Evans AT, Chaffee A, Bender G, Johnston J, Muir W, Blanchard G. Ebstein's anomaly: a report of 3 cases in the dog. J Am Vet Med Assoc. 1977 Apr 1; 170(7): 709-13.
29. Robertson SA, Eyster G, Perry R, Patterson V. Surgical palliation of severe tricuspid valve stenosis in a dog by use of Fontan's procedure. Vet Surg. 1999 Sep-Oct; 28(5): 368-74.
30. Brown WA, Thomas WP. Balloon valvuloplasty of tricuspid stenosis in a Labrador retriever. J Vet Intern Med. 1995 Nov-Dec; 9(6): 419-24.
31. Kunze P, Abbott JA, Hamilton SM, Pyle RL. Balloon valvuloplasty for palliative treatment of tricuspid stenosis with right-to-left atrial level shunting in a dog. J Am Vet Med Assoc. 2002 Feb 15; 220(4): 491-6, 464.
32. Takemura N, Machida N, Nakagawa K, Amasaki H, Washizu M, Hirose H. Ebstein's anomaly in a beagle dog. J Vet Med Sci. 2003 Apr; 65(4): 531-3.
33. Choi R, Lee SK, Moon HS, Park IC, Hyun C. Ebstein's anomaly with an atrial septal defect in a jindo dog. Can Vet J. 2009 Apr; 50(4): 405-10.
34. Guglielmini C, Diana A, Pietra M, Cipone M. Atrial septal defect in five dogs. J Small Anim Pract. 2002 Jul; 43(7): 317-22.
35. Chetboul V, Trolle JM, Nicolle A, Carlos Sampedrano C, Gouni V, Laforge H,

Benalloul T, Tissier R, Pouchelon JL. Congenital heart diseases in the boxer dog: a retrospective study of 105 cases (1998-2005). J Vet Med A Physiol Pathol Clin Med. 2006 Sep; 53(7): 346-51.
36. Chetboul V, Charles V, Nicolle A, Sampedrano CC, Gouni V, Pouchelon JL, Tissier R. Retrospective study of 156 atrial septal defects in dogs and cats (2001-2005). J Vet Med A Physiol Pathol Clin Med. 2006 May; 53(4): 179-84.
37. Garcia-Rodriguez MB, Granja MA, Garcia CC, Gonzalo Orden JM, Cano Rabano MJ, Prieto ID. Complex cardiac congenital defects in an adult dog: an ultrasonographic and magnetic resonance imaging study. Can Vet J. 2009 Sep; 50(9): 933-5.
38. Sanders RA, Hogan DE, Green HW 3rd, Hoyer MH, Puppel DA. Transcatheter closure of an atrial septal defect in a dog. J Am Vet Med Assoc. 2005 Aug 1; 227(3): 430-4.
39. Gordon SG, Miller MW, Roland RM, Saunders AB, Achen SE, Drourr LT, Nelson DA. Transcatheter atrial septal defect closure with the Amplatzer atrial septal occluder in 13 dogs: short- and mid-term outcome. J Vet Intern Med. 2009 Sept-Oct; 23 (5): 995-1002.
40. Gordon SG, Nelson DA, Achen SE, Miller MM, Roland RM, Saunders AB, Drourr LT. Open heart closure of an atrial septal defect by use of an atrial septal occluder in a dog. J Am Vet Med Assoc. 2010 Feb 15; 236(4): 434-9.
41. Raush WP, Keene BW. Spontaneous resolution of an isolated ventricular septal defect in a dog. J Am Vet Med Assoc. 2003 Jul 15; 223(2): 219-20.
42. Thomas WP. Echocardiographic diagnosis of congenital membranous ventricular septal aneurysm in the dog and cat. J Am Anim Hosp Assoc. 2005 Jul-Aug;41(4):215-20.
43. Shimizu M, Tanaka R, Hoshi K, Hirao H, Kobayashi M, Shimamura S, Yamane Y. Surgical correction of ventricular septal defect with aortic regurgitation in a dog. Aust Vet J. 2006 Apr;84(4):117-21.
44.Shimizu M, Tanaka R, Hirao H, Kobayashi M, Shimamura S, Maruo K, Yamane Y. Percutaneous transcatheter coil embolization of a ventricular septal defect in a dog. J Vet Med Sci. 2004 May;66(5):559-62.
45.Bussadori C, Carminati M, Domenech O. Transcatheter closure of a perimembranous ventricular septal defect in a dog. J Vet Intern Med. 2007 Nov-Dec;21(6):1396-400.
46. Margiocco ML, Bulmer BJ, Sisson DD. Percutaneous occlusion of a muscular ventricular septal defect with an Amplatzer muscular VSD occluder. J Vet Cardiol. 2008 Jun;10(1):61-6.
47. Leib A, Lang J, Lombard CW. Eisenmenger syndrome in a 9-month-old border collie puppy. Schweiz Arch Tierheilkd. 1998; 140(4): 164-7.
48. Patterson DF, Pyle RL, Van Mierop L, Melbin J, Olson M. Hereditary defects of the conotruncal septum in keeshond dogs: pathologic and genetic studies. Am J Cardiol. 1974 Aug;34(2):187-205.
49. Patterson DF, Pexieder T, Schnarr WR, Navratil T, Alaili R. A single major-gene defect underlying cardiac conotruncal malformations interferes with myocardial growth during embryonic development: studies in the CTD line of keeshond dogs. Am J Hum Genet. 1993 Feb;52(2):388-97.
50. Werner P, Raducha MG, Prociuk U, Budarf M, Henthorn PS, Patterson DF. Comparative mapping of the DiGeorge region in the dog ad exclusion of linkage to inherited canine conotruncal heart defects. J Hered. 1999 Jul-Aug;90(4):494-8.

51. Werner P, Raducha MG, Prociuk U, Ostrander EA, Spielman RS, Kirkness EF, Patterson DF, Henthorn PS. The keeshond defect in cardiac conotruncal development is oligogenic. Hum Genet. 2005 Apr; 116(5): 368-77.
52. Eyster GE, Braden TD, Appleford M, et al. Surgical management of tetralogy of Fallot. J Small Anim Pract 1977; 18 :387-394
53. Brockman DJ, Holt DE, Gaynor JW, Theman TE. Long-term palliation of tetralogy of Fallot in dogs by use of a modified Blalock-Taussig shunt. J Am Vet Med Assoc. 2007 Sep 1; 231(5): 721-6.
54. Oguchi Y, Matsumoto H, Masuda Y, Takashima H, Takashima K, Yamane Y. Balloon dilation of right ventricular outflow tract in a dog with tetralogy of Fallot. J Vet Med Sci. 1999 Sep; 61(9): 1067-9.
55. Lew LJ, Fowler JD, McKay R, Egger CM, Rosin MW. Open-heart correction of tetralogy of Fallot in an acyanotic dog. J Am Vet Med Assoc. 1998 Sep 1; 213(5): 652-7.
56. Orton EC, Mama K, Hellyer P, Hackett TB. Open surgical repair of tetralogy of Fallot in dogs. J Am Vet Med Assoc. 2001 Oct 15; 219(8): 1089-93, 1073.
57. Legendre AM, Appleford MD, Eyster GE, Dade AW. Secondary polycythemia and seizures due to right to left shunting patent ductus arteriosus in a dog. J Am Vet Med Assoc. 1974 Jun 15; 164(12): 1198-1201.
58. Pyle RL, Park RD, Alexander AF, Hill BL. Patent ductus arteriosus with pulmonary hypertension in the dog. J Am Vet Med Assoc. 1981 Mar 15; 178(6): 565-71.
59. O'Brien SE, Riedesel EA, Myers RK, Riedesel DH. Right-to-left patent ductus arteriosus with dysplastic left ventricle in a dog. J Am Vet Med Assoc. 1988 May 15; 192(10): 1435-8.
60. Arora M. Reversed patent ductus arteriosus in a dog. Can Vet J. 2001 Jun; 42(6): 471-2.
61. Anderson TP, Walker MC, Goring RL. Cardiogenic hypertrophic osteopathy in a dog with a right-to-left shunting patent ductus arteriosus. J Am Vet Med Assoc. 2004 May 1; 224(9): 1464-6, 1453.
62. Jenni SD, Vogt P, Jenni R, Glaus TM. Dissection of a patent ductus arteriosus with right heart failure in an adult dog. J Vet Intern Med. 2007 May-Jun; 21(3): 526-30.
63. Ferasin L, Rizzo F, Darke PG. Original investigation of right-to-left shunting patent ductus arteriosus in an Irish setter puppy. Vet J. 2007 Mar; 173(2): 443-8.
64. Morandi F, Daniel GB, Gompf RE, Bahr A. Diagnosis of congenital cardiac right-to-left shunts with 99mTc-macroaggregated albumin. Vet Radiol Ultrasound. 2004 Mar-Apr; 45(2): 97-102.
65. Seibert RL, Maisenbacher HW 3rd, Prosek R, Adin DB, Arsenault WG, Estrada AH. Successful closure of left-to-right patent ductus arteriosus in three dogs with concurrent pulmonary hypertension. J Vet Cardiol. 2010 Apr; 12(1): 67-73.
66. Côté E, Ettinger SJ. Long-term clinical management of right-to-left ("reversed") patent ductus arteriosus in 3 dogs. J Vet Intern Med. 2001Jan-Feb; 15(1): 39-42.
67. Moore KW, Stepien RL. Hydroxyurea for treatment of polycythemia secondary to right-to-left shunting patent ductus arteriosus in 4 dogs. J Vet Intern Med. 2001 Jul-Aug; 15(4):418-21.
68. Basso C, Fox PR, Meurs KM, Towbin JA, Spier AW, Calabrese F, Maron BJ, Thiene G. Arrhythmogenic right ventricular cardiomyopathy causing sudden cardiac death in boxer dogs: a new animal model of human disease. Circulation. 2004 Mar 9;109(9):1180-

5.
69. Stern JA, Meurs KM, Spier AW, Koplitz SL, Baumwart RD. Ambulatory electrocardiographic evaluation of clinically normal adult Boxers. J Am Vet Med Assoc. 2010 Feb 15;236(4):430-3.
70. Scansen BA, Meurs KM, Spier AW, Koplitz S, Baumwart RD. Temporal variability of ventricular arrhythmias in Boxer dogs with arrhythmogenic right ventricular cardiomyopathy. J Vet Intern Med. 2009 Sep-Oct;23(5):1020-4.
71. Baumwart RD, Meurs KM, Raman SV. Magnetic resonance imaging of right ventricular morphology and function in boxer dogs with arrhythmogenic right ventricular cardiomyopathy. J Vet Intern Med. 2009 Mar-Apr;23(2):271-4.
72. Meurs KM, Mauceli E, Lahmers S, Acland GM, White SN, Lindblad-Toh K. Genome-wide association identifies a deletion in the 3' untranslated region of striatin in a canine model of arrhythmogenic right ventricular cardiomyopathy. Hum Genet. 2010 Sep;128(3):315-24.
73. Meurs KM, Ederer MM, Stern JA. Desmosomal gene evaluation in Boxers with arrhythmogenic right ventricular cardiomyopathy. Am J Vet Res. 2007 Dec;68(12):1338-41.
74. Oyama MA, Reiken S, Lehnart SE, Chittur SV, Meurs KM, Stern J, Marks AR. Arrhythmogenic right ventricular cardiomyopathy in Boxer dogs is associated with calstabin2 deficiency. J Vet Cardiol. 2008 Jun;10(1):1-10.
75. Fernández del Palacio MJ, Bernal LJ, Bayón A, Bernabé A, Montes de Oca R, Seva J. Arrhythmogenic right ventricular dysplasia/cardiomyopathy in a Siberian husky. J Small Anim Pract. 2001 Mar;42(3):137-42.
76. Santilli RA, Bontempi LV, Perego M, Fornai L, Basso C. Outflow tract segmental arrhythmogenic right ventricular cardiomyopathy in an English Bulldog. J Vet Cardiol. 2009 Jun;11(1):47-51.
77. Simonneau G, Robbins IM, Beghetti M, Channick RN, Delcroix M, Denton CP, Elliott CG, Gaine SP, Gladwin MT, Jing ZC, Krowka MJ, Langleben D, Nakanishi N, Souza R. Updated clinical classification of pulmonary hypertension. J Am Coll Cardiol. 2009 Jun 30;54(1 Suppl):S43-54.
78. Kolm US, Amberger CN, Boujon CE, Lombard CW. Plexogenic pulmonary arteriopathy in a Pembroke Welsh corgi. J Small Anim Pract. 2004 Sep;45(9):461-6.
79. Zabka TS, Campbell FE, Wilson DW. Pulmonary arteriopathy and idiopathic pulmonary arterial hypertension in six dogs. Vet Pathol. 2006 Jul;43(4):510-22.
80. Russell NJ, Irwin PJ, Hopper BJ, Olivry T, Nicholls PK. Acute necrotizing pulmonary vasculitis and pulmonary hypertension in a juvenile dog. J Small Anim Pract. 2008 Jul;49(7):349-55.
81. Glaus TM, Soldati G, Maurer R, Ehrensperger F. Clinical and pathological characterisation of primary pulmonary hypertension in a dog. Vet Rec. 2004 Jun 19;154(25):786-9.
82. Serres FJ, Chetboul V, Tissier R, Carlos Sampedrano C, Gouni V, Nicolle AP, Pouchelon JL. Doppler echocardiography-derived evidence of pulmonary arterial hypertension in dogs with degenerative mitral valve disease: 86 cases (2001-2005). J Am Vet Med Assoc. 2006 Dec 1;229(11):1772-8.

83. Chiavegato D, Borgarelli M, D'Agnolo G, Santilli RA. Pulmonary hypertension in dogs with mitral regurgitation attributable to myxomatous valve disease. Vet Radiol Ultrasound. 2009 May-Jun;50(3):253-8.
84. Corcoran BM, Cobb M, Martin MW, Dukes-McEwan J, French A, Fuentes VL, Boswood A, Rhind S. Chronic pulmonary disease in West Highland white terriers. Vet Rec. 1999 May 29;144(22):611-6.
85. Heikkilä HP, Lappalainen AK, Day MJ, Clercx C, Rajamäki MM. Clinical, Bronchoscopic, Histopathologic, Diagnostic Imaging, and Arterial Oxygenation Findings in West Highland White Terriers with Idiopathic Pulmonary Fibrosis. J Vet Intern Med. 2011 Mar 2.
86. Webb JA, Armstrong J. Chronic idiopathic pulmonary fibrosis in a West Highland white terrier. Can Vet J. 2002 Sep;43(9):703-5.
87. Norris AJ, Naydan DK, Wilson DW. Interstitial lung disease in West Highland White Terriers. Vet Pathol. 2005 Jan;42(1):35-41.
88. Goggs R, Benigni L, Fuentes VL, Chan DL. Pulmonary thromboembolism. J Vet Emerg Crit Care (San Antonio). 2009 Feb;19(1):30-52. Review.89. Hirano Y, Kitagawa H, Sasaki Y. Relationship between pulmonary arterial pressure and pulmonary thromboembolism associated with dead worms in canine heartworm disease. J Vet Med Sci. 1992 Oct;54(5):897-904
90. Ninomiya H, Wakao Y. Scanning electron microscopy of vascular corrosion casts and histologic examination of pulmonary microvasculature in dogs with dirofilariosis. Am J Vet Res. 2002 Nov;63(11):1538-44.
91. Uchide T, Saida K. Elevated endothelin-1 expression in dogs with heartworm disease. J Vet Med Sci. 2005 Nov;67(11):1155-61.
92. Nicolle AP, Chetboul V, Tessier-Vetzel D, Carlos Sampedrano C, Aletti E, Pouchelon JL. Severe pulmonary arterial hypertension due to Angiostrongylosus vasorum in a dog. Can Vet J. 2006 Aug;47(8):792-5.
93. Bertazzolo W, Zuliani D, Pogliani E, Caniatti M, Bussadori C. Diffuse bronchiolo-alveolar carcinoma in a dog. J Small Anim Pract. 2002 Jun;43(6):265-8.
94. Lord PF and Suter PF. Radiology. In Fox PR, Sisson DD, and Moïse NS (eds). Textbook of Canine and Feline Cardiology: Principles and Clinical Practice, 2nd ed. Saunders: Philadelphia 1999. 107-129.
95. Lehmkuhl LB, Bonagura JD, Biller DS, Hartman WM. Radiographic evaluation of caudal vena cava size in dogs. Vet Radiol Ultrasound. 1997 Mar-Apr;38(2):94-100.
96. Carlsson C, Häggström J, Eriksson A, Järvinen AK, Kvart C, Lord P. Size and shape of right heart chambers in mitral valve regurgitation in small-breed dogs. J Vet Intern Med. 2009 Sep-Oct;23(5):1007-13.
97. Spier AW, Meurs KM. Use of signal-averaged electrocardiography in the evaluation of arrhythmogenic right ventricular cardiomyopathy in boxers. J Am Vet Med Assoc. 2004 Oct 1;225(7):1050-5.
98. Moïse NS and Fox PR. Echocardiography and Doppler Imaging. In Fox PR, Sisson DD, and Moïse NS (eds). Textbook of Canine and Feline Cardiology: Principles and Clinical Practice, 2nd ed. Saunders: Philadelphia 1999. 130-171.
99. Foale R, Nihoyannopoulos P, McKenna W, et al. Echocardiographic measurement of the normal adult right ventricle. Br Heart J 1986;56:33-44.

100. Rudski LG, Lai WW, Afilalo J, Hua L, Handschumacher MD, Chandrasekaran K, Solomon SD, Louie EK, Schiller NB. Guidelines for the echocardiographic assessment of the right heart in adults: a report from the American Society of Echocardiography endorsed by the European Association of Echocardiography, a registered branch of the European Society of Cardiology, and the Canadian Society of Echocardiography. J Am Soc Echocardiogr. 2010 Jul;23(7):685-713
101. Skinner JR, Stuart AG, O'Sullivan J, Heads A, Boys RJ, Hunter S. Right heart pressure determination by Doppler in infants with tricuspid regurgitation. Arch Dis Child. 1993 Aug;69(2):216-20.
102. Skinner JR, Boys RJ, Heads A, Hey EN, Hunter S. Estimation of pulmonary arterial pressure in the newborn: study of the repeatability of four Doppler echocardiographic techniques. Pediatr Cardiol. 1996 Nov-Dec;17(6):360-9.
103. Stephen B, Dalal P, Berger M, Schweitzer P, Hecht S. Noninvasive estimation of pulmonary artery diastolic pressure in patients with tricuspid regurgitation by Doppler echocardiography. Chest. 1999 Jul;116(1):73-7.
104. Lanzarini L, Fontana A, Lucca E, Campana C, Klersy C. Noninvasive estimation of both systolic and diastolic pulmonary artery pressure from Doppler analysis of tricuspid regurgitant velocity spectrum in patients with chronic heart failure. Am Heart J. 2002 Dec;144(6):1087-94.
105. Ghio S, Raineri C, Scelsi L, Recusani F, D'armini AM, Piovella F, Klersy C, Campana C, Viganò M, Tavazzi L. Usefulness and limits of transthoracic echocardiography in the evaluation of patients with primary and chronic thromboembolic pulmonary hypertension. J Am Soc Echocardiogr. 2002 Nov;15(11):1374-80.
106. Miller D, Farah MG, Liner A, Fox K, Schluchter M, Hoit BD. The relation between quantitative right ventricular ejection fraction and indices of tricuspid annular motion and myocardial performance. J Am Soc Echocardiogr. 2004 May;17(5):443-7.
107. Hsiao SH, Lin SK, Wang WC, Yang SH, Gin PL, Liu CP. Severe tricuspid regurgitation shows significant impact in the relationship among peak systolic tricuspid annular velocity, tricuspid annular plane systolic excursion, and right ventricular ejection fraction. J Am Soc Echocardiogr. 2006 Jul;19(7):902-10.
108. Johnson L, Boon J, Orton EC. Clinical characteristics of 53 dogs with Doppler-derived evidence of pulmonary hypertension: 1992-1996. J Vet Intern Med. 1999 Sep-Oct;13(5):440-7.
109. Schober KE, Baade H. Doppler echocardiographic prediction of pulmonary hypertension in West Highland white terriers with chronic pulmonary disease. J Vet Intern Med. 2006 Jul-Aug;20(4):912-20.
110. Serres F, Chetboul V, Gouni V, Tissier R, Sampedrano CC, Pouchelon JL. Diagnostic value of echo-Doppler and tissue Doppler imaging in dogs with pulmonary arterial hypertension. J Vet Intern Med. 2007 Nov-Dec;21(6):1280-9.
111. Cook RA, Carnes G, Lee TY, Wells RG. Respiration-averaged CT for attenuation correction in canine cardiac PET/CT. J Nucl Med. 2007 May;48(5):811-8.
112. Tsai IC, Huang JL, Ueng KC, Hung YW, Hung CF, Liao WC, Lei HY, Chen MC, Tsai WL, Chen SA, Chen CC, Fu YC, Ting CT. Global and regional wall motion abnormalities of pacing-induced heart failure assessed by multi-detector row CT: a patient and canine model study. Int J Cardiovasc Imaging. 2010 Dec;26(Suppl 2):223-35.

113. Hockings PD, Busza AL, Byrne J, Patel B, Smart SC, Reid DG, Lloyd HL, White A, Pointing K, Farnfield BA, Criado-Gonzalez A, Whelan GA, Taylor GL, Birmingham JM, Slaughter MR, Osborne JA, Krebs-Brown A, Templeton D. Validation of MRI measurement of cardiac output in the dog: the effects of dobutamine and minoxidil. Toxicol Mech Methods. 2003;13(1):39-43.
114. Shors SM, Fung CW, François CJ, Finn JP, Fieno DS. Accurate quantification of right ventricular mass at MR imaging by using cine true fast imaging with steady-state precession: study in dogs. Radiology. 2004 Feb;230(2):383-8.
115. Sacks MS, Chuong CJ, Templeton GH, Peshock R. In vivo 3-D reconstruction and geometric characterization of the right ventricular free wall. Ann Biomed Eng. 1993 May-Jun;21(3):263-75.
116. Gilbert SH, McConnell FJ, Holden AV, Sivananthan MU, Dukes-McEwan J. The potential role of MRI in veterinary clinical cardiology. Vet J. 2010 Feb;183(2):124-34.
117. Baumwart RD, Meurs KM, Raman SV. Magnetic resonance imaging of right ventricular morphology and function in boxer dogs with arrhythmogenic right ventricular cardiomyopathy. J Vet Intern Med. 2009 Mar-Apr;23(2):271-4.
118. García-Rodríguez MB, Granja MA, García CC, Gonzalo Orden JM, Cano Rábano MJ, Prieto ID. Complex cardiac congenital defects in an adult dog: an ultrasonographic and magnetic resonance imaging study. Can Vet J. 2009 Sep;50(9):933-5.
119. Mai W, Weisse C, Sleeper MM. Cardiac magnetic resonance imaging in normal dogs and two dogs with heart base tumor. Vet Radiol Ultrasound. 2010 Jul-Aug;51(4):428-35.
120. Sisson D, Schaeffer D. Changes in linear dimensions of the heart, relative to body weight, as measured by M-mode echocardiography in growing dogs. Am J Vet Res. 1991 Oct; 52(10): 1591-6.
121. Cornell CC, Kittleson MD, Della Torre P, Häggström J, Lombard CW, Pedersen HD, Vollmar A, Wey A. Allometric scaling of M-mode cardiac measurements in normal adult dogs. J Vet Intern Med. 2004 May-Jun; 18(3): 311-21.
122. Hall DJ, Cornell CC, Crawford S, Brown DJ. Meta-analysis of normal canine echocardiographic dimensional data using ratio indices. J Vet Cardiol. 2008 Jun; 10(1): 11-23.
123. Brown DJ, Rush JE, MacGregor J, Ross JN Jr, Brewer B, Rand WM. M-mode echocardiographic ratio indices in normal dogs, cats, and horses: a novel quantitative method. J Vet Intern Med. 2003 Sep-Oct; 17(5): 653-62.
124. Gonçalves AC, Orton EC, Boon JA, Salman MD. Linear, logarithmic, and polynomial models of M-mode echocardiographic measurements in dogs. Am J Vet Res. 2002 Jul; 63(7): 994-9.
125. Neilan TG, Pradhan AD, Weyman AE. Derivation of a size-independent variable for scaling of cardiac dimensions in a normal adult population. J Am Soc Echocardiogr. 2008 Jul; 21(7): 779-85.
126. Neilan TG, Pradhan AD, King ME, Weyman AE. Derivation of a size-independent variable for scaling of cardiac dimensions in a normal paediatric population. Eur J Echocardiogr. 2009 Jan; 10(1): 50-5.
127. George K, Sharma S, Batterham A, Whyte G, McKenna W. Allometric analysis of the association between cardiac dimensions and body size variables in 464 junior athletes. Clin Sci (Lond). 2001 Jan;100(1):47-54.

128. Batterham AM, George KP, Mullineaux DR. Allometric scaling of left ventricular mass by body dimensions in males and females. Med Sci Sports Exerc. 1997 Feb;29(2):181-6.
129. Simpson KE, Craig Devine B, Gunn-Moore DA, et al. Assessment of the repeatability of feline echocardiography using conventional echocardiography and spectral pulse-wave doppler tissue imaging techniques. Veterinary Radiology & Ultrasound 2007;48:58-68.
130. Dukes-McEwan J, French A, Corcoran B. Doppler echocardiography in the dog: measurement variability and reproducibility. Veterinary Radiology & Ultrasound 2002;43:144-152.
131 Buhl R, Ersbøll AK, Eriksen L, Koch J. Sources and magnitude of variation of echocardiographic measurements in normal standardbred horses. Vet Radiol Ultrasound. 2004 Nov-Dec;45(6):505-12.
132. Gabriel RS, Bakshi TK, Scott AG, Christiansen JP, Patel H, Wong SP, Armstrong GP. Reliability of echocardiographic indices of dyssynchrony. Echocardiography. 2007 Jan;24(1):40-6.
133 Vandenberg BF, Ayres RW, Lindower PD, Burns TL, Kerber RE. Reproducibility and variability of the amount of tricuspid regurgitation with color Doppler echocardiography. Am J Cardiol. 1995 Jul 15;76(3):198-9.
134. Clark RD, Korcuska K, Cohn K. Serial echocardiographic evaluation of left ventricular function in valvular disease, including reproducibility guidelines for serial studies. Circulation 1980;62:564-575.
135. Jones G and Barker A. Reference intervals. Clin Biochem Rev 2008: 29 (supplement): S93-S97.
136. Chetboul V, Tidholm A, Nicolle A, Sampedrano CC, Gouni V, Pouchelon JL, Lefebvre HP, Concordet D. Effects of animal position and number of repeated measurements on selected two-dimensional and M-mode echocardiographic variables in healthy dogs. J Am Vet Med Assoc. 2005 Sep 1;227(5):743-7.
137. Schwarzwald CC, Schober KE, Bonagura JD. Methods and reliability of echocardiographic assessment of left atrial size and mechanical function in horses. Am J Vet Res. 2007 Jul;68(7):735-47.
138. Serres F, Chetboul V, Tissier R, Gouni V, Desmyter A, Sampedrano CC, Pouchelon JL. Quantification of pulmonary to systemic flow ratio by a Doppler echocardiographic method in the normal dog: Repeatability, reproducibility, and reference ranges. J Vet Cardiol. 2009 Jun;11(1):23-9.
139. Bland JM and Altman DG. Measuring agreement in method comparison studies. Stat Methods Med Res 1999; 8: 135-160.
140. Bercovitz, A, Moss A, Sengupta, M, Park-Lee EY, Jones A, Harris-Kojetin, LD. An overview of home health aides: United States 2007. Health Statistics Reports 2011, May 19; 34: 1-32.
141. Chetboul V, Athanassiadis N, Carlos C, Nicolle A, Zilberstein L, Pouchelon JL, Lefebvre HP, Concordet D. Assessment of repeatability, reproducibility, and effect of anesthesia on determination of radial and longitudinal left ventricular velocities via tissue Doppler imaging in dogs. Am J Vet Res. 2004 Jul;65(7):909-15.
142. Chetboul V, Sampedrano CC, Gouni V, Concordet D, Lamour T, Ginesta J, Nicolle

AP, Pouchelon JL, Lefebvre HP. Quantitative assessment of regional right ventricular myocardial velocities in awake dogs by Doppler tissue imaging: repeatability, reproducibility, effect of body weight and breed, and comparison with left ventricular myocardial velocities. J Vet Intern Med. 2005 Nov-Dec;19(6):837-44.
143. Wess G, Killich M, Hartmann K. Comparison of pulsed wave and color Doppler myocardial velocity imaging in healthy dogs. J Vet Intern Med. 2010 Mar-Apr;24(2):360-6.
144. Chetboul V, Concordet D, Pouchelon JL, Athanassiadis N, Muller C, Benigni L, Munari AC, Lefebvre HP. Effects of inter- and intra-observer variability on echocardiographic measurements in awake cats. J Vet Med A Physiol Pathol Clin Med. 2003 Aug;50(6):326-31.
145. Simpson KE, Devine BC, Gunn-Moore DA, French AT, Dukes-McEwan J, Koffas H, Moran CM, Corcoran BM. Assessment of the repeatability of feline echocardiography using conventional echocardiography and spectral pulse-wave Doppler tissue imaging techniques. Vet Radiol Ultrasound. 2007 Jan-Feb;48(1):58-68.

Echocardiographic Assessment of the Canine Right Heart:
Reference Intervals and Repeatability, Phases 1 and 2

Abstract

Objectives: *Phase 1)* Establish echocardiographic reference intervals for measurements of the normal canine right heart. *Phase 2)* Describe the repeatability of normal right heart echocardiographic measurements.

Materials and Methods: *Phase 1)* 45 healthy adult dogs. Dogs underwent one echocardiographic examination by the same operator. *Phase 2)* 6 randomly selected dogs from the pool of Phase 1 dogs. Dogs underwent repeated echocardiograms by two operators.

Results: *Phase 1*) The linear relationship between dimension and transformed body weight was highly variable. For linear dimensions, most of the scaling exponents were close to the theoretical value of 1/3. For area measurements, most of the scaling exponents were close to 2/3. *Phase 2)* Of the 168 within-day, between-day and between-operator coefficients of variation (CV) generated, 154 (91.7%) were below 15% and 135 (80.4%) were less than 10%. The analysis of variance revealed the operator to be a significant source of variation for 28 of 42 measurements.

Conclusions: The right heart can be measured with relatively low repeatability. The right atrium can be imaged from either the right parasternal long axis or left parasternal four-chamber views. The right ventricle is best imaged from the left parasternal four-chamber plane. The caudal vena cava can also be assessed from a modified four-chamber view. The left parasternal short axis provides for repeatable measurement of the right ventricular outflow tract and main pulmonary artery. The pulmonic valve and aortic valve dimensions and ratio were repeatable in the right parasternal short axis view.

Introduction

The canine right heart is directly or indirectly affected by numerous congenital and acquired cardiac diseases. In fact, the right heart is affected in approximately 68% of dogs with congenital cardiac disease[1,2] and approximately 61% of dogs with acquired cardiac disease[1]. In addition, pulmonary hypertension from non-cardiac causes including thromboembolism, pulmonary disease, and arteriopathies can also affect the right heart, although the prevalence of pulmonary hypertension in the canine population has not been published. Echocardiography is non-invasive and provides details on the structure, function and hemodynamics of the right and left heart. In dogs, image planes for right heart echocardiography have not been fully defined, nor have comprehensive prediction intervals for measurements of the right heart.

Echocardiographic image planes suited to the assessment of the human right heart have been standardized and prediction intervals for quantitative variables published.[3] Additionally, echocardiography has been validated for the estimation of pulmonary artery pressure in neonates[4,5] and adults.[6,7] Echocardiographic indices of myocardial function have also been shown to significantly correlate with thermodilution-derived right ventricular ejection fraction.[8] Prediction intervals for right heart measurements obtained from humans have been derived using allometric scaling. Prediction intervals developed in this way are an alternative to intervals that are based on a presumed linear relationship between echocardiographic variables and measured or calculated indices of body size such as body weight or body surface area. Allometric scaling has been shown to be superior to other forms of indexing in children[9], teenage athletes[10] and adults[11].

We attempted to define standard echocardiographic image planes of the canine right heart through systematic examination of healthy dogs. Allometric scaling was used to define the relationship between quantitative echocardiographic variables and body size. From these relationships, prediction intervals were developed. In addition, a study subsample was randomly selected and subject to repeated echocardiographic examination. Intra-operator and inter-operator measurement variability was evaluated in order to define limits of measurement repeatability.

Materials and Methods

Animals

This study was approved by the Institutional Animal Care and Use Committee (IACUC) of Virginia Tech. Healthy adult dogs of both sexes were recruited from faculty and staff of the Virginia-Maryland Regional College of Veterinary Medicine (VMRCVM). Dogs were considered to be healthy on the basis of physical examination and patient history. All dogs were receiving heartworm preventative and/or had been shown within the last six months to be free of Dirofilaria antigenemia using a commercially available ELISA. Dogs were excluded if the history disclosed thyroid disease or if abnormalities of the cardiovascular system were detected by physical examination. The dogs were recruited so that approximately equal numbers of dogs fit into the following weight categories: 1-25 lbs. (0.45-11.36kg), 26-50 lbs. (11.81-22.72kg), 51-75 lbs. (23.18-34.09kg), 76-100 lbs (34.54-45.45kg). Table 1 describes the zoographic characteristics of these dogs. Boxer dogs and dogs of presumed Boxer dog lineage were excluded because of the apparently high prevalence of arrhythmogenic right ventricular cardiomyopathy in dogs of this breed. Prior to data collection, standard echocardiographic images were subjectively evaluated; dogs were excluded if this preliminary examination was abnormal or if the simultaneously recorded electrocardiogram disclosed arrhythmia.

Experimental Design

Phase 1. Forty-five dogs underwent echocardiographic examination by the same operator (JMG). All echocardiograms were done within a two week period

Phase 2. Of the dogs from Phase 1, six were randomly selected to investigate repeatability of echocardiographic dimensions and indices. These six dogs underwent repeated echocardiograms by two operators (JMG and JAA) twice daily (morning and afternoon) on three non-consecutive days (Monday, Wednesday and Friday of one week). Thus, each dog was echocardiographically examined 12 times. The echocardiographic protocol described below was used for all examinations.

Echocardiography

Transthoracic echocardiography was performed using an ultrasound unit[a] equipped with probes that house multifrequency phased-array transducers. The choice of carrier frequency and variables that determine image characteristics was at the discretion of the operator and was consistent during Phase 2.

Each animal was gently restrained in right and then, left lateral recumbency without the use of sedation. M-mode and 2D images were obtained from the right and left parasternal positions. Image planes were identified and measurements were taken according to the recommendations of the American Society of Echocardiography.[12-14] An electrocardiogram was simultaneously recorded during image capture.

The measurements were taken as shown in Figures 1-8. Measurements were taken off-line from digitally saved images using offline measurement software[b]. Measurements were taken from a minimum of five, usually consecutive, cardiac cycles and then averaged. Measurements were taken of: right atrial linear dimensions and area,

right ventricular wall thicknesses, right ventricular internal dimensions and area, right ventricular outflow tract dimensions, diameter of pulmonic valve hinge points, main pulmonary artery dimensions, and aortic valve/ascending aorta dimensions. For 2D images in which the tricuspid valve was visible, end-diastole was defined as the first frame in which tricuspid valve was closed. For M-mode images or images in which the tricuspid valve was not visible, end-diastole was determined electrocardiographically and was defined as the onset of the QRS. End-systole was the frame that immediately preceded tricuspid valve opening. Except where noted – see figure legends – a leading edge to leading edge convention was used for measurement of M-mode images. For 2D images, an inner edge to inner edge convention was used for lumenal dimensions. For measurement of wall thickness, the endocardial border furthest from the transducer was included but the more proximal was not.

Statistical Analysis

Phase 1: A logarithmic (base 10) transformation was applied to the data followed by linear regression with log body weight as the predictor. The slope of the regression line gives the constant b in the allometric equation, and the antilogarithm ($\log^{-1}$) of the intercept gives the constant a.[15] Log Normal M-mode averages and prediction intervals were generated. For the prediction component of the analysis a representative list of body weights were included in the dataset. The model was used to obtain constants (on the log scale) for indexing M-mode variables to calculate prediction intervals for arbitrary body weights.[15] For each regression, residual plots were inspected to verify model adequacy.

Phase 2: Coefficients of variation were generated for time within day (for each operator), day to day (for each operator), and operator to operator variation. Fixed effects for operator, day, and time of day were assessed using mixed model ANOVA. Besides the three fixed effects, the mixed model also included dog as a random effect. For all ANOVA models, residual plots were inspected to verify model adequacy. Statistical significance was set $\alpha=0.05$. All analyses were performed using SAS version 9.2.[c]

Figure 1. Right parasternal short-axis M-mode of the right ventricle. Measurements were made using the leading edge-to-leading edge convention. End-diastolic measurements were taken at the onset of the QRS complex and systolic measurements were taken at the point of maximal excursion of the interventricular septum.

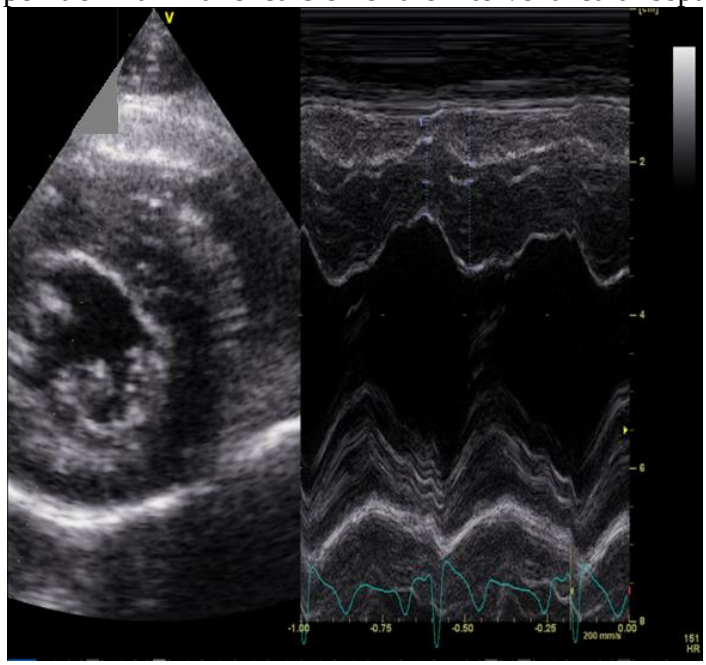

Figure 2. Right parasternal short-axis image of the heart base showing the aortic valve and pulmonic valve. Measurements were taken from inside edge-to-inside edge and at the onset of diastole from the first frame in which the valve leaflets were seen to be closed.

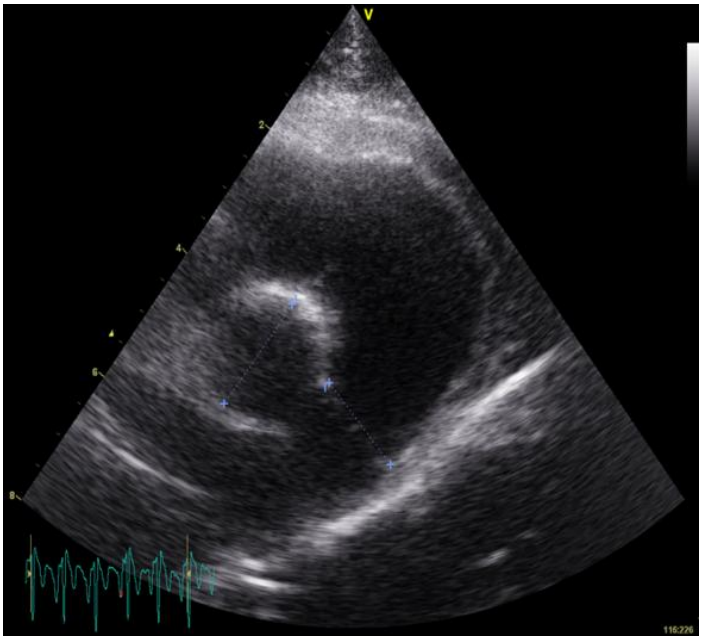

Figure 3. Right parasternal long-axis image of the right ventricle. End-diastolic measurements were taken leading edge-to-leading edge. End-diastolic measurements were taken from the first frame after tricuspid valve closure and systolic measurements were taken from the frame that immediately preceded tricuspid valve opening. Measurements were positioned at mid-ventricular level just basilar to the papillary muscle if visualized.

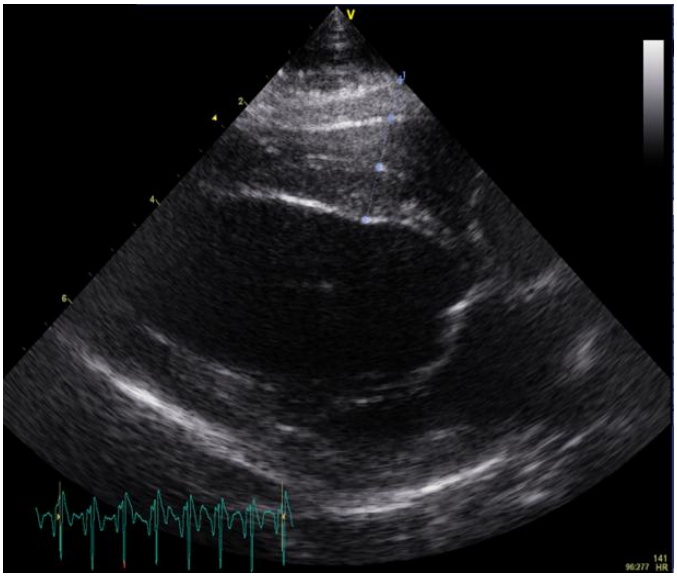

Figure 4. Modified right parasternal long-axis image intended to optimize the view of the right atrium. Measurements were taken inside edge-to-inside edge and taken at end-

systole from the frame that immediately preceded tricuspid valve opening.

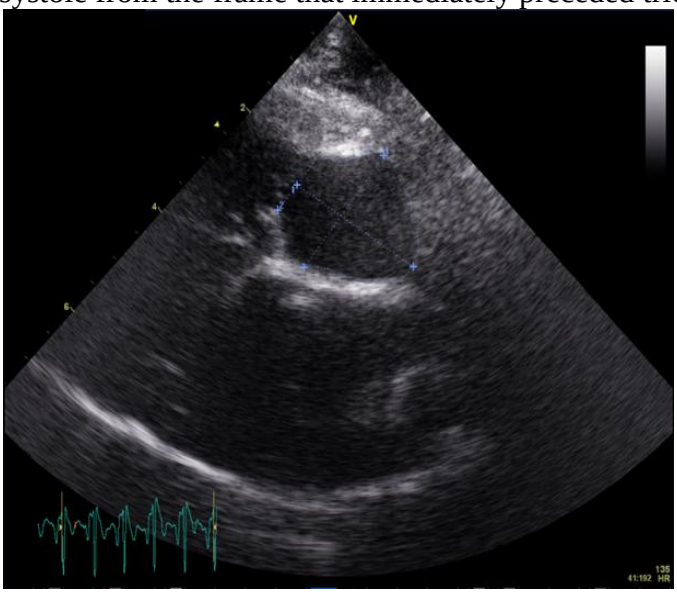

Figure 5. Left parasternal four-chamber view optimized for the right ventricular inflow. Measurements were made inside edge-to-inside edge and area was traced along the inside edge of the chamber. End-diastolic measurements were taken from the first frame in which tricuspid valve closure was visible. End-systolic measurements were taken from the frame that immediately preceded tricuspid valve opening.

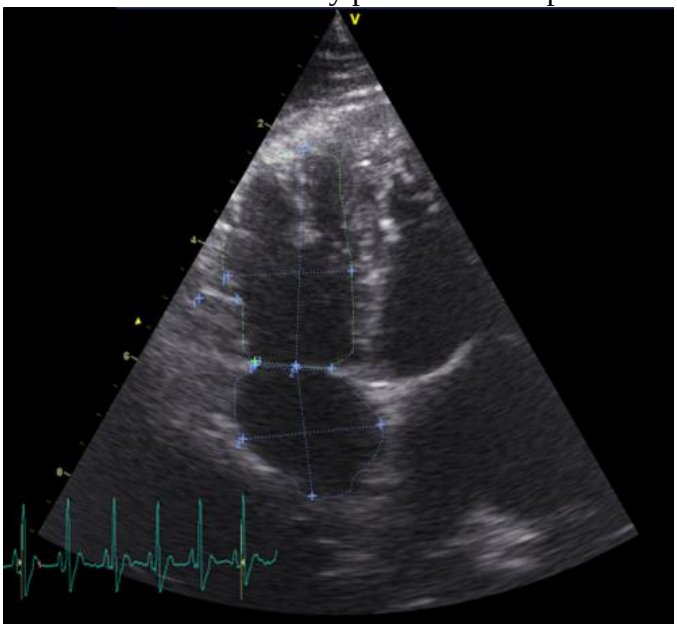

Figure 6. A left parasternal four-chamber view was used to direct the M-mode cursor through the lateral tricuspid valve annulus. Measurement of tricuspid annular place systolic excursion was taken as the difference between peak diastolic and peak systolic position.

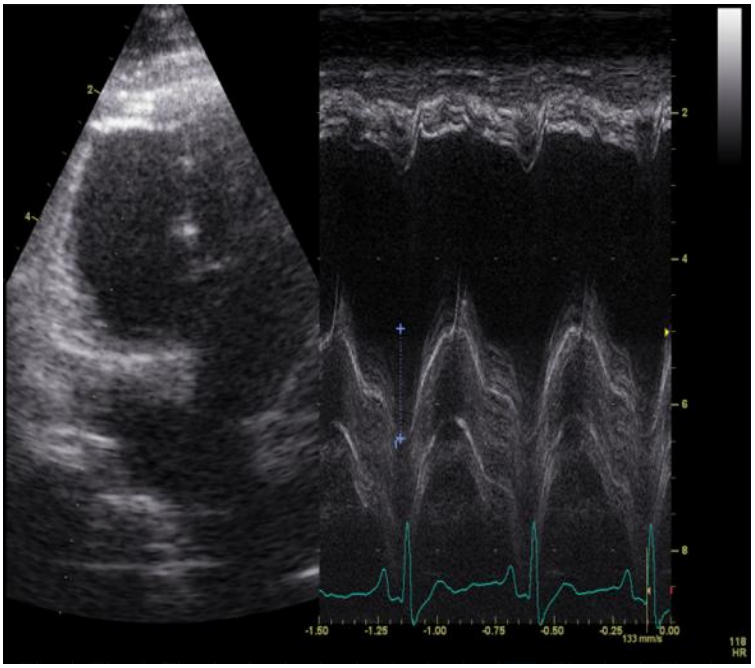

Figure 7. Left parasternal four-chamber view optimized for visualization of the caudal vena cava. The measurement was taken from the frame that immediately preceded tricuspid valve opening at the furthest point from the right atrium where the cava could still be visualized.

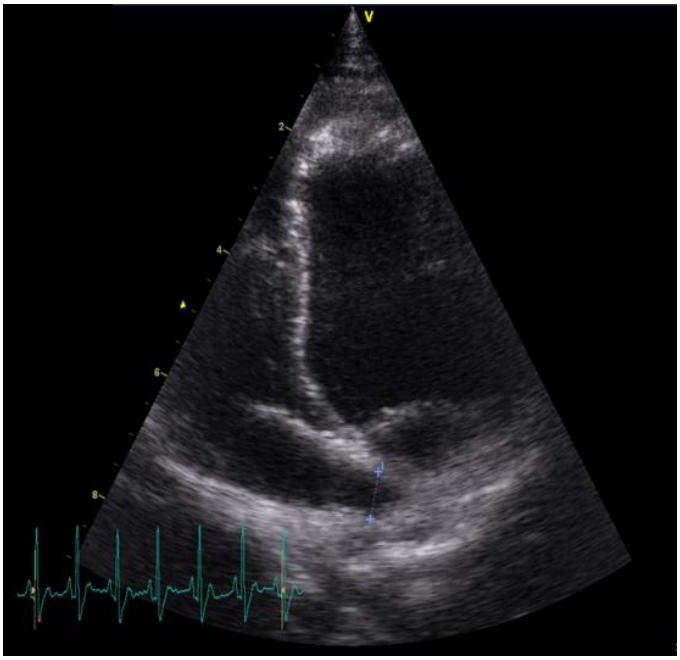

Figure 8. Left parasternal short-axis image. Measurements were taken from inside edge-to-inside edge of the right ventricular outflow tract, pulmonic valve and main pulmonary artery just proximal to its bifurcation. Measurements were taken from the first frame in which pulmonic valve closure was visible. M-mode: cursor was positioned through the

RVOT and the center of the aortic valve. Measurements were taken leading edge-to-leading edge at the onset of the QRS.

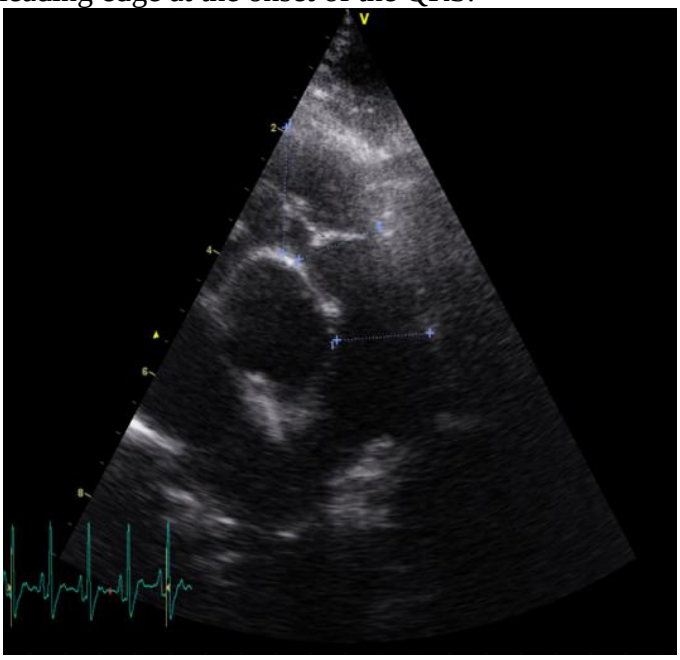

[a] Vivid 7 Dimension, GE Healthcare, Waukesha WI

[b] EchoPAC dimension v.6.1.x, GE Healthcare Technologies, Milwaukee, WI, USA

[c] SAS, version 9.2, Carey NC, USA

Results

Of the 45 dogs that were recruited for phase 1, three were excluded: one for mitral regurgitation, one for moderately severe tricuspid regurgitation and one for an accelerated idioventricular rhythm. From the remaining 42 dogs, 6 were randomly selected for the second phase. The zoographic characteristics of the dogs are summarized in Table 1.

Phase 1

Linear regression equations that describe the relationship between $\log_{10}$ body weight and $\log_{10}$ of each linear dimension are listed in Table 2. As expected, statistically significant linear relationships between body-weight and the dimensionless indices, % fractional shortening – obtained from either M-mode or 2D images – and fractional area change of the right ventricle, were not detected. With the exceptions of end-systolic right ventricular internal minor dimensions from both M-mode and 2D images, there was a statistically significant ($p<0.05$) linear relationship between body-weight and all other recorded echocardiographic variables. The strength of the linear relationship was highly variable; the range of coefficients of determination (R^2) was 0.0545-0.8719. For linear dimensions, the scaling exponent of derived allometric equations ranged between 0.135122 and 0.390771; most were close to the theoretical value of 1/3. For measurements of chamber area, scaling exponents ranged between 0.583709 and 0.71363 and were close to 2/3.

Phase 2

Of the 168 CV generated, (Table 3a), 135 (80.4%) were less than 10% and 154 (91.7%) were below 15%. Of the 33 CV that were greater than 10%, 18 belonged to operator 1 (9 within-day and 9 between-day) and 15 belonged to operator 2 (9 within-day and 6 between-day). The significant ($p<0.05$) fixed effects of operator, day or time of day are listed in Table 3b. The analysis of variance revealed the operator to be a significant ($p<0.05$) source of variation for 28 of 42 measurements.

From the data, predictions intervals were developed for the most repeatable or notable measurements for varying body weights (Tables 4-8).

Table 1: Zoographic characteristics of the healthy dogs.

Characteristic	Phase 1 dogs	Phase 2 dogs
Age (years)	5.8 ± 3.5	4.9 ± 2.7
Sex Female Male	 Spayed (22), Intact (0) Neutered (20), Intact (0)	 Spayed (4), Intact (0) Neutered (2), Intact (0)
Body weight (kg)	22.8 ± 12.3	18.2 ± 9.7
Body surface area (cm^2)	0.77 ± 0.3	0.67 ± 0.2
Breed (number)	1-25lbs group: - Jack Russell Terrier (2) - Border Terrier (1) - Corgi (1) - Mix breed (4) - Dachshund (2) 26-50lbs group: - Collie (1) - Border Collie (1) - Miniature Poodle (2) - Mix breed (6) - Jack Russell Terrier (1) 51-75lbs group: - Labrador (5) - Greyhound (1) - Australian Shepherd (1) - Doberman Pinscher (2) - Mix breed (2) 76-100lbs group: - Malamute (1) - Golden Retriever (3) - Labrador (1) - Mix breed (3) - German Shepherd Dog (1) - Greyhound (1)	1-25lbs group: - Jack Russell Terrier (1) - Mixed Breed (1) 26-50lbs group: - Jack Russell Terrier (1) - Mixed Breed (1) 51-75lbs group: - Labrador retriever (2) 76-100lbs group: - none

Table 2: Summary of measurement regression equations and statistics.

Phase 1		
Measurement	Regression equation	R^2
2D right parasternal short axis		
Pulmonic valve diameter (PV_R_sax)	0.824953+0.301491*logBW	0.7853
Aortic valve diameter (AV_R_sax)	0.822407+0.356122*logBW	0.8619
Pulmonic valve to Aortic valve ratio (PV_AV_ratio_R_ sax)	(-).017811-0.041798*logBW	0.0981
2D right parasternal long axis		
Right ventricular free wall in diastole (RVFWd_R_lax)	0.390873+0.275452*logBW	0.5037
Right ventricular internal dimension in diastole (RVIDd_R_lax)	0.861872+0.148513*logBW	0.1245
Interventricular septum in diastole (IVSd_R_lax)	0.435586+0.344324*logBW	0.5991
Right ventricular free wall in systole (RVFWs_R_lax)	0.507303+0.259724*logBW	0.5472
Right ventricular internal dimension in systole (RVIDs_R_lax)	0.76929+0.135122*logBW	0.0688
Interventricular septum in systole (IVSs_R_lax)	0.652662+0.254046*logBW	0.5240
Fractional shortening (FS_R_lax)	1.236852+.015262*logBW	0.0001
Right atrial major dimension (RA Major_R_lax)	1.060494+0.282667*logBW	0.4355
Right atrial minor dimension (RA Minor_R_lax)	1.00999+0.275307*logBW	0.4033
Right atrial area (RA_area_R_lax)	1.949974+0.583709*logBW	0.7340
2D left parasternal four-chamber		
Right ventricular free wall in diastole (RVFWd_L4ch)	0.498702+0.254182*logBW	0.5945
Right ventricular major dimension in diastole (RVd_Major_L4ch)	1.154135+0.304162*logBW	0.6119
Right ventricular minor dimension in diastole (RVd_Minor_L4ch)	0.846215+0.326954*logBW	0.5467
Tricuspid valve annular dimension in diastole (TVAd_L4ch)	0.735034+0.337273*logBW	0.4784
Right ventricular free wall in systole (RVFWs_L4ch)	0.519731+0.286221*logBW	0.6182
Right ventricular major dimension in systole (RVs_Major_L4ch)	1.013676+0.328402*logBW	0.7194
Right ventricular minor dimension in systole (RVs_Minor_L4ch)	0.735578+0.310655*logBW	0.4295
Tricuspid valve annular dimension in systole (TVAs_L4ch)	0.688756+0.318396*logBW	0.5832
Right ventricular area in diastole (RVd_area_L4ch)	1.961878+0.623833*logBW	0.7222
Right ventricular area in systole (RVs_area_L4ch)	1.729135+0.624347*logBW	0.6471

Right ventricular fractional area change (FAC_L4ch)	1.579882+.014655*logBW	0.0017
Right atrial major dimension (RA Major_L4ch)	0.977159+0.324407*logBW	0.7944
Right atrial minor dimension (RA Minor_L4ch)	0.871147+0.390771*logBW	0.7895
Right atrial area (RA_area_L4ch)	1.768113+0.71363*logBW	0.8719
Caudal vena cava diameter (CdVC_L4ch)	0.591306+0.245228*logBW	0.4604
2D left parasternal short axis		
Right ventricular outflow tract (RVOT_L_sax)	1.025462+0.207539*logBW	0.3167
Pulmonic valve diameter (PV_L_sax)	0.844638+0.269217*logBW	0.7602
Main pulmonary artery diameter (MPA_L_sax)	0.72956+0.329011*logBW	0.7949
M-mode right parasternal short axis		
Right ventricular free wall in diastole (RVFWd_R_sax_M)	0.321412+0.269231*logBW	0.4664
Right ventricular internal dimension in diastole (RVIDd_R_sax_M)	0.717061+0.156588*logBW	0.0545
Interventricular septum in diastole (IVSd_R_sax_M)	0.618252+0.251863*logBW	0.5423
Right ventricular free wall in systole (RVFWs_R_sax_M)	0.551412+0.253287*logBW	0.6414
Right ventricular internal dimension in systole (RVIDs_R_sax_M)	0.62828+0.190164*logBW	0.0606
Interventricular septum in systole (IVSs_R_sax_M)	0.748007+0.233537*logBW	0.1486
Fractional shortening (FS_R_sax_M)	1.201233-.001197*logBW	0.000
M-mode left parasternal four-chamber		
Tricuspid annular plane systolic excursion (TAPSE_L4ch_M)	0.779385+0.236224*logBW	0.4318
M-mode left parasternal short axis		
Right ventricular outflow tract dimension (RVOT_L_sax_M)	1.147835+0.168088*logBW	0.2995
Aortic valve diameter (AV_L_sax_M)	0.942538+0.301405*logBW	0.7673
Right ventricular outflow tract dimension to aortic valve diameter ratio (RVOT_AV_ratio_L_sax_M)	.205418-.133413*logBW	0.1676

Table 3a. Coefficients of variation, with values greater than 10% in bold.

	Operator 1	Operator 2	Operator 1	Operator 2	CV between-operator (%)
	CV within-day (%)		CV between-day (%)		
PV_R_sax	3.7	4.1	2.4	3.1	4.9
AV_R_sax	2.4	4.5	2.4	5.3	5.3
PV_AV_ratio_R_ sax	3.1	5.0	2.2	3.1	5.2
RVFWd_R_lax	**10.7**	5.8	9.8	7.1	**13.7**
RVIDd_R_lax	8.8	7.1	**10.2**	6.2	**16.1**
IVSd_R_lax	5.8	4.9	3.8	4.5	6.8
RVFWs_R_lax	9.1	6.4	**11.2**	6.9	**11.1**
RVIDs_R_lax	**13.2**	**13.2**	**12.4**	9.3	**21.3**
IVSs_R_lax	4.2	7.5	3.2	4.4	7.5
FS_R_lax	**25.6**	**33.7**	**17.2**	**18.4**	**33.6**
RA Major_R_lax	4.2	4.4	1.7	3.6	6.2
RA_Minor_R_lax	4.0	8.4	3.5	7.5	**10.4**
RA_area_R_lax	6.9	9.6	4.2	8.7	**11.4**
RVFWd_L4ch	8.5	8.5	8.6	6.3	**12.0**
RVd_Minor_L4ch	6.5	6.4	6.4	5.7	8.2
TVAd_L4ch	5.4	7.5	7.2	5.4	**25.6**
RVd_Major_L4ch	2.9	3.5	3.3	1.5	3.4
RVFWs_L4ch	8.2	6.5	8.2	5.2	**12.7**
RVs_Minor_L4ch	**10.4**	6.4	9.7	9.1	**11.0**
TVAs_L4ch	9.1	4.8	8.3	5.5	**17.5**
RVs_Major_L4ch	4.7	3.5	4.6	3.5	4.6
RVd_area_L4ch	6.0	8.2	6.2	4.1	8.7
RVs_area_L4ch	8.5	7.2	8.8	8.3	8.8
FAC_L4ch	5.8	**10.4**	6.3	8.7	**11.1**
RA_Major_L4ch	3.4	3.6	6.3	2.9	6.4
RA_Minor_L4ch	3.6	7.6	7.1	8.6	9.8
RA_area_L4ch	7.0	8.4	9.8	9.5	**11.9**
CdVC_L4ch	7.5	**12.9**	5.6	7.1	**11.4**
RVOT_L_sax	8.0	5.4	6.7	5.2	7.8
PV_hingepoints_ L_sax	4.3	5.4	3.1	5.5	6.2
MPA_L_sax	4.7	5.4	3.7	4.5	8.2
RVFWd_R_sax_M	**10.9**	**14.5**	**12.5**	8.0	**18.5**
RVIDd_R_sax_M	**19.5**	**20.8**	**17.0**	**17.7**	**24.1**
IVSd_R_sax_M	5.3	9.5	6.7	9.1	8.9
RVFWs_R_sax_M	8.2	**10.1**	**11.8**	6.3	**13.4**
RVIDs_R_sax_M	**21.2**	**21.4**	**21.6**	**15.6**	**30.2**
IVSs_R_sax_M	6.5	8.1	4.1	8.4	8.3
FS_R_sax_M	**21.1**	**86.2**	4.4	**10.7**	**44.3**
TAPSE_L4ch_M	**10.8**	8.1	**14.1**	**11.5**	**21.0**
RVOT_L_sax_M	5.6	5.1	4.5	7.6	**12.5**
AV_L_sax_M	5.1	5.0	3.8	7.8	6.0
RVOT_AV_ratio_ L_sax_M	8.4	8.1	4.9	**11.8**	**16.2**

Table 3b. Significant ANOVA fixed effects

	Significant ANOVA Fixed effect
PV_R_sax	-
AV_R_sax	Operator
PV_AV_ratio_R_ sax	Operator, time
RVFWd_R_lax	Operator, day
RVIDd_R_lax	Operator
IVSd_R_lax	Operator
RVFWs_R_lax	Operator
RVIDs_R_lax	Operator
IVSs_R_lax	Operator
FS_R_lax	-
RA Major_R_lax	Operator
RA_Minor_R_lax	Operator, day
RA_area_R_lax	Operator
RVFWd_L4ch	Operator
RVd_Minor_L4ch	-
TVAd_L4ch	Operator
RVd_Major_L4ch	-
RVFWs_L4ch	Operator
RVs_Minor_L4ch	-
TVAs_L4ch	Operator
RVs_Major_L4ch	-
RVd_area_L4ch	Operator
RVs_area_L4ch	Day
FAC_L4ch	Operator
RA_Major_L4ch	-
RA_Minor_L4ch	Operator, day
RA_area_L4ch	-
CdVC_L4ch	-
RVOT_L_sax	Operator
PV_hingepoints_L_sax	Operator
MPA_L_sax	Operator
RVFWd_R_sax_M	Operator
RVIDd_R_sax_M	-
IVSd_R_sax_M	Day
RVFWs_R_sax_M	Operator, day
RVIDs_R_sax_M	-
IVSs_R_sax_M	Operator, day
FS_R_sax_M	Operator
TAPSE_L4ch_M	Operator
RVOT_L_sax_M	Operator
AV_L_sax_M	-
RVOT_AV_ratio_L_sax_M	Operator

Table 4. Right parasternal short axis mean values and prediction intervals

Body wt.	PV mm	AV mm	PV:AV
3	9.3 (7.3 – 11.9)	9.8 (7.9 – 12.2)	0.9 (0.8-1.1)
4	10.2 (8.0 – 12.9)	10.9 (8.8-13.5)	0.9 (0.7-1.1)
6	11.5 (9.1 – 14.4)	12.6 (10.2-15.5)	0.9 (0.7-1.1)
9	13.0 (10.3 – 16.3)	14.5 (11.8-17.8)	0.9 (0.7-1.1)
11	13.8 (11.0 – 17.2)	15.6 (12.7-19.1)	0.9 (0.7-1.0)
15	15.1 (12.1 – 18.9)	17.4 (14.2-21.3)	0.9 (0.7-1.0)
20	16.5 (13.2 – 20.6)	19.3 (15.8-23.6)	0.8 (0.7-1.0)
25	17.6 (14.1 – 22.1)	20.9 (17.1-25.6)	0.8 (0.7-1.0)
30	18.6 (14.9 – 23.3)	22.3 (18.2-27.3)	0.8 (0.7-1.0)
35	19.5 (15.6 – 24.5)	23.6 (19.2-28.9)	0.8 (0.7-1.0)
40	20.3 (16.2 – 25.5)	24.7 (20.1-30.3)	0.8 (0.7-1.0)
50	21.7 (17.3 – 27.3)	26.8 (21.8-32.9)	0.8 (0.7-1.0)
60	23.0 (18.2 – 28.9)	28.6 (23.2-35.2)	0.8 (0.7-1.0)
70	24.1 (19.1 – 30.4)	30.2 (24.4-37.2)	0.8 (0.7-1.0)

Table 5. Right parasternal long axis mean values and prediction intervals

Body wt.	RA Major mm	RA Minor mm	RA Area mm^2
3	15.7 (9.6-25.7)	13.8 (8.3-23.1)	169.2 (98.7-290.1)
4	17.0 (10.5-27.6)	15.0 (9.1-24.8)	200.2 (118.1-339.2)
6	19.1 (11.9-30.6)	16.8 (10.3-27.4)	253.6 (151.6-424.2)
9	21.4 (13.5-34.0)	18.7 (11.6-30.3)	321.4 (194.0-532.4)
11	22.6 (14.3-35.8)	19.8 (12.3-31.9)	361.3 (218-596.7)
15	24.7 (15.7-39.0)	21.6 (13.4-34.7)	433.0 (263.0-713.0)
20	26.8 (17.0-42.3)	23.3 (14.5-37.5)	512.2 (311.2-842.8)
25	28.6 (18.1-45.1)	24.8 (15.4-39.9)	583.4 (354.2-961.0)
30	30.1 (19.0-27.6)	26.1 (16.2-42.1)	648.9 (393.3-1070.8)
35	31.4 (19.8-49.8)	27.2 (16.9-44.0)	710.0 (429.4-1174.1)
40	32.6 (20.5-51.8)	28.3 (17.5-45.7)	767.6 (463.1-1272.2)
50	34.7 (21.8-55.4)	30.0 (18.5-48.8)	874.4 (525.0-1456.2)
60	36.6 (22.8-58.6)	31.6 (19.3-51.6)	972.6 (581.2-1627.5)
70	38.2 (23.7-61.5)	33.0 (20.1-54.1)	1064.1 (632.9-1789.0)

Table 6a. Left parasternal four-chamber mean values and prediction intervals

Body wt.	RVFWd mm	RVFWs mm	RVd Minor mm	RVs Minor mm	TVAd mm	TVAs mm
3	4.2 (3.0-5.8)	4.5 (3.2-6.4)	10.1 (6.4-15.9)	7.7 (4.4-13.3)	7.9 (4.6-13.5)	6.9 (4.6-10.5)
4	4.5 (3.3-6.1)	4.9 (3.5-6.9)	11.0 (7.1-17.3)	8.4 (4.9-14.3)	8.7 (5.1-14.7)	7.6 (5.1-11.4)
6	5.0 (3.7-6.8)	5.5 (4.0-7.7)	12.6 (8.2-19.5)	9.5 (5.6-16.0)	9.9 (5.9-16.6)	8.6 (5.8-12.8)
9	5.5 (4.1-7.5)	6.2 (4.5-8.6)	14.4 (9.4-22.1)	10.8 (6.4-18.0)	11.4 (6.9-18.9)	9.8 (6.7-14.5)
11	5.8 (4.3-7.8)	6.6 (4.8-9.1)	15.4 (10.0-23.5)	11.5 (6.9-19.10	12.2 (7.4-20.2)	10.5 (7.1-15.4)
15	6.3 (4.7-8.5)	7.2 (5.2-9.9)	17.0 (11.1-26.0)	12.6 (7.6-21.0)	13.5 (8.2-22.3)	11.6 (7.9-16.9)
20	6.8 (5.0-9.1)	7.8 (5.7-10.7)	18.7 (12.3-28.5)	13.8 (8.3-22.9)	14.9 (9.1-24.6)	12.7 (8.7-18.6)
25	7.1 (5.3-9.6)	8.3 (6.0-11.4)	20.1 (13.2-30.7)	14.8 (8.9-24.6)	16.1 (9.8-26.5)	13.6 (9.3-19.9)
30	7.5 (5.5-10.1)	8.8 (6.4-12.1)	21.3 (14.0-32.6)	15.6 (9.4-26.1)	17.7 (10.4-28.3)	14.4 (9.8-21.2)
35	7.8 (5.8-10.5)	9.2 (6.6-12.6)	22.4 (14.7-34.4)	16.4 (9.8-27.4)	18.0 (10.9-29.8)	15.1 (10.3-22.3)
40	8.1 (6.0-10.9)	9.5 (6.9-13.1)	23.4 (15.3-36.0)	17.1 (10.2-28.60	18.9 (11.4-31.3)	15.8 (10.7-23.3)
50	8.5 (6.3-11.6)	10.1 (7.3-14.1)	25.2 (16.4-38.90	18.3 (10.9-30.8)	20.3 (12.2-33.9)	17.0 (11.5-25.1)
60	8.9 (6.6-12.1)	10.7 (7.7-14.9)	26.8 (17.3-41.4)	19.4 (11.5-32.8)	21.6 (12.9-36.2)	18.0 (21.1-26.7)
70	9.3 (6.8-12.7)	11.2 (8.0-15.6)	28.1 (18.1-43.7)	20.4 (12.0-34.6)	22.8 (13.5-38.3)	18.9 (12.7-28.1)

Table 6b. Left parasternal four-chamber mean values and prediction intervals

Body wt.	RVd Major mm	RVs Major mm	RVd Area mm2	RVs Area mm2	RV FAC %
3	19.9 (13.7-28.9)	14.8 (10.8-20.3)	181.8 (100.4-329.1)	106.4 (52.5-215.9)	40.7 (38.0-43.5)
4	21.7 (15.1-31.3)	16.3 (12.0-22.10	217.5 (121.7-388.8)	127.4 (63.7-254.5)	40.7 (38.0-43.5)
6	24.6 (17.3-35.1)	18.6 (13.8-25.1)	280.1 (159.0-493.5)	164.0 (83.5-322.1)	40.7 (38.0-43.5)
9	27.8 (19.6-39.4)	21.2 (15.8-28.5)	360.7 (206.9-628.9)	211.3 (108.9-409.8)	40.7 (38.0-43.5)
11	29.6 (20.9-41.8)	22.7 (16.9-30.4)	408.8 (235.3-710.3)	239.5 (124.0-462.6)	40.7 (38.0-43.5)
15	32.5 (23.0-45.8)	25.1 (18.8-33.6)	496.1 (286.5-859.1)	290.7 (151.1-559.3)	40.7 (38.0-43.5)
20	35.5 (25.2-50.0)	27.6 (20.6-36.9)	593.6 (343.0-1027.3)	347.9 (181.0-668.8)	40.7 (38.0-43.5)
25	38.0 (26.9-53.5)	29.7 (22.2-39.7)	682.3 (393.8-1182.1)	399.9 (207.7-769.7)	40.7 (38.0-43.5)
30	40.1 (28.4-56.7)	31.5 (23.5-42.2)	764.5 (440.4-1327.0)	448.1 (232.3-864.5)	40.7 (38.0-43.5)
35	42.1 (29.7-59.5)	33.2 (24.7-44.5)	841.6 (483.7-1464.3)	493 (255.0-954.5)	40.7 (38.0-43.5)
40	43.8 (30.9-62.0)	34.7 (25.8-46.5)	914.7 (524.4-1595.6)	536.3 (276.4-1040.6)	40.7 (38.0-43.5)
50	46.9 (33.0-66.6)	37.3 (27.7-50.2)	1051.4 (599.6-1843.6)	616.4 (315.7-1203.7)	40.7 (38.0-43.5)
60	49.5 (34.7-70.7)	39.6 (29.3-53.5)	1178.0 (668.2-2076.6)	690.7 (351.5-1357.4)	40.7 (38.0-43.5)
70	51.9 (36.6-74.3)	41.6 (30.8-56.4)	1296.9 (731.9-2298.0)	760.5 (384.7-1503.7)	40.7 (38.0-43.5)

Table 6c. Left parasternal four-chamber mean values and prediction intervals

Body wt.	RA Major mm	RA Minor mm	RA Area mm2	CdVC mm
3	13.6 (10.5-17.5)	11.4 (8.4-15.6)	128.4 (84.4-195.3)	5.1 (3.4-7.7)
4	14.9 (11.6-19.1)	12.8 (9.4-17.3)	157.7 (104.6-237.7)	5.5 (3.7-8.2)
6	17.0 (13.3-21.60	15.0 (11.1-20.1)	210.6 (141.1-314.3)	6.1 (4.1-8.9)
9	19.4 (15.3-24.5)	17.5 (13.1-23.4)	281.2 (189.9-416.6)	6.7 (4.6-9.8)
11	20.7 (16.3-26.1)	19.0 (14.2-25.3)	324.6 (219.6-479.6)	7.0 (4.8-10.3)
15	22.8 (18.1-28.9)	21.4 (16.1-28.5)	405.0 (274.7-597.0)	7.6 (5.2-11.0)
20	25.1 (19.8-31.7)	24.0 (18.0-31.9)	497.2 (337.4-732.8)	8.1 (5.6-11.9)
25	27.0 (21.3-34.1)	26.1 (19.6-34.8)	583.1 (395.4-859.9)	8.6 (5.9-12.5)
30	28.6 (22.6-36.2)	28.1 (21.1-37.4)	664.1 (449.7-980.7)	9.0 (6.2-13.1)
35	30.1 (23.7-38.1)	29.8 (22.3-39.8)	741.3 (501.2-1096.6)	9.3 (6.4-13.6)
40	31.4 (24.8-39.8)	31.4 (23.5-42.0)	815.4 (550.3-1208.3)	9.6 (6.6-14.1)
50	33.8 (26.6-42.9)	34.3 (25.6-45.9)	956.2 (642.9-1422.2)	10.2 (6.9-15.0)
60	35.8 (28.1-45.6)	36.8 (27.4-49.5)	1089.1 (729.5-1625.9)	10.7 (7.2-15.7)
70	37.6 (29.5-48.0)	39.1 (29.0-52.7)	1215.7 (811.4-1821.6)	11.1 (7.5-16.4)

Table 7. Left parasternal short axis mean values and prediction intervals

Body wt.	RVOT mm	PV mm	MPA mm
3	13.3 (8.3-21.3)	9.4 (7.5-11.90)	7.7 (6.0-10.0)
4	14.1 (8.9-22.3)	10.2 (8.1-12.7)	8.5 (6.6-10.9)
6	15.4 (9.8-24.0)	11.3 (9.1-14.1)	9.7 (7.6-12.4)
9	16.7 (10.8-25.9)	12.6 (10.2-15.7)	11.1 (8.7-14.1)
11	17.4 (11.3-27.0)	13.3 (10.7-16.5)	11.8 (9.3-15.0)
15	18.6 (12.1-28.7)	14.5 (11.7-18.0)	13.1 (10.3-16.6)
20	19.7 (12.8-30.4)	15.7 (12.6-19.4)	14.4 (11.3-18.2)
25	20.7 (13.4-31.9)	16.6 (13.4-20.6)	15.5 (12.2-19.6)
30	21.5 (13.9-33.2)	17.5 (14.1-21.7)	16.4 (12.9-20.8)
35	22.2 (14.3-34.3)	18.2 (14.7-22.6)	17.3 (13.6-22.0)
40	22.8 (14.7-35.3)	18.9 (15.2-23.5)	18.1 (14.2-23.0)
50	24.8 (15.9-38.8)	20.0 (16.1-25.0)	19.4 (15.2-24.8)
60	24.8 (15.9-38.8)	21.1 (16.9-26.3)	20.6 (16.2-26.4)
70	25.6 (16.3-40.2)	21.9 (17.5-27.4)	21.7 (17.0-27.8)

Table 8. Left parasternal short axis M-mode mean values and prediction intervals

Body wt.	TAPSE mm	RVOT mm	AV mm	RVOT:AV
3	7.8 (5.1-11.8)	16.9 (11.4-25.1)	12.2 (9.5-15.7)	1.1 (1.0-1.2)
4	8.3 (5.6-12.5)	17.7 (12.1-26.1)	13.3 (10.4-17.1)	1.1 (1.0-1.2)
6	9.2 (6.2-13.7)	19.0 (13.0-27.7)	15.0 (11.8-19.2)	1.1 (1.0-1.2)
9	10.1 (6.9-14.9)	20.3 (14.1-29.4)	17.0 (13.4-21.6)	1.1 (1.0-1.2)
11	10.6 (7.2-15.6)	21.0 (14.6-30.4)	18.0 (14.2-22.9)	1.1 (1.0-1.2)
15	11.4 (7.8-16.8)	22.2 (15.4-31.9)	19.8 (15.7-25.1)	1.1 (1.0-1.2)
20	12.2 (8.3-17.9)	23.3 (16.2-33.5)	21.6 (17.1-27.3)	1.1 (1.0-1.2)
25	12.9 (8.8-18.9)	24.1 (16.8-34.8)	23.1 (18.3-29.3)	1.1 (1.0-1.2)
30	13.4 (9.1-19.8)	24.9 (17.3-35.9)	24.4 (19.3-30.9)	1.1 (1.0-1.2)
35	13.9 (9.5-20.5)	25.5 (17.7-36.9)	25.6 (20.2-32.4)	1.1 (1.0-1.2)
40	14.4 (9.7-21.2)	26.1 (18.1-37.8)	26.6 (21.0-33.8)	1.1 (1.0-1.2)
50	15.2 (10.2-22.5)	27.1 (18.7-39.4)	28.5 (22.4-36.20	1.1 (1.0-1.2)
60	15.8 (10.6-23.5)	28.0 (19.2-40.8)	30.1 (23.6-38.4)	1.1 (1.0-1.2)
70	16.4 (11.0-24.5)	28.7 (19.6-42.0)	31.5 (24.7-40.3)	1.1 (1.0-1.2)

Discussion

This study is the first to define standard imaging planes for echocardiographic assessment of the canine right heart. The imaging planes and measurements were similar to those proposed by the American Society of Echocardiography in 2010 and used in human cardiology. With adequate understanding of the planes, the images were not difficult to obtain and could be easily adopted by trained veterinary echocardiographers. The ultimate goal of this study was the determination of the echo-derived measurement means, prediction intervals and repeatability estimates which could be applied to clinical cases and clinical research related to diseases of the right heart.

Means and prediction intervals for different body weights were calculated for each measurement using allometric scaling. The decision to use allometric scaling was based on previous veterinary and human studies that showed linear echocardiographic measurements do not have a linear relationship with body weight or body surface area. In previous veterinary studies, linear echocardiographic dimensions were linearly related to body weight raised to an exponent that was generally between 0.25 and 0.33. Our echocardiographic dimensions and body-weights were subject to $\log_{10}$ transformation. A statistically significant linear relationship between log transformed body-weight and echocardiographic dimension was detected for all but six measurements – half of those being M-mode measurements taken from the right parasternal short axis view.

The repeatability arm of this study described the least and most repeatable approaches to echocardiographic evaluation of the right heart. Values for the CVs ranged from 1.5% to 86.2% with 195 of the 210 calculated CVs below 20%. Previous studies of

the repeatability of left heart measurements have found measurements to be fairly repeatable with the majority of measurements having associated CVs below 15%[16] or 20%[17]. Our study produced a wider range of CVs than these studies, but the vast majority, 93%, remained below 20%. Most of the CVs over 20% were from the "between operator" column, indicating that comparison studies are ideally performed and measured by the same operator. Based on the findings of our study we recommend imaging the right atrium from either the right parasternal long axis or left parasternal four-chamber views. The right ventricle is best imaged from the left parasternal four-chamber plane. The caudal vena cava can also be assessed from a modified four-chamber view. The left parasternal short axis provides repeatable measurement of the right ventricular outflow tract and main pulmonary artery. The pulmonic valve and aortic valve dimensions and ratio were repeatable in the right parasternal short axis view. Interestingly, our recommendations are similar to those put forth by the American Society of Echocardiographer in their guidelines for the echocardiographic evaluation of the right heart. They recommend imaging the right atrium from the left four-chamber plane. They also recommend that the right ventricular free wall thickness and the right ventricular lumen be assessed in the four-chamber view. The distal right ventricular outflow tract should be assessed from the left parasternal short-axis view. The function of the right ventricle should be assessed using one of the following methods: FAC, TAPSE, tissue Doppler systolic velocity of the tricuspid valve annulus and RIMP (more commonly known in the veterinary field as the Tei index). We found FAC to have CVs less than 11.2% and TAPSE was just slightly less repeatable with CVs between 8-21%. Tissue doppler evaluation of the tricuspid valve annulus has been previously described

and documented to have a within-day CV of10% and between-day CV of 15.5%.[18] Additionally the Tei index has been previously shown to accurately reflect right ventricular function.[19]

Limitations of this study include a lack of "gold standard" measurement technique to which this echocardiographic technique could be compared. In addition, several breeds were included but the study sample is not a representation of all known breeds.

Future areas of study include: the duplication of this study using boxer dogs alone, to obtain breed-specific prediction intervals for a breed that is predisposed to arrhythmogenic right ventricular cardiomyopathy; duplication of the repeatability arm using dogs with identifiable but stable right heart disease; and application of the prediction intervals to clinical patients.

References

1. Buchanan JW. Prevalence of cardiovascular diseases. In Fox PR, Sisson DD, and Moïse NS (eds). Textbook of Canine and Feline Cardiology: Principles and Clinical Practice, 2nd ed. Saunders: Philadelphia 1999. 457-470.
2. Oliveira P, Domenech O, Silva J, Vannini S, Bussadori R, Bussadori C. Retrospective review of congenital heart disease in 976 dogs. J Vet Intern Med. 2011 May;25(3):477-83.
3. Rudski LG, Lai WW, Afilalo J, Hua L, Handschumacher MD, Chandrasekaran K, Solomon SD, Louie EK, Schiller NB. Guidelines for the echocardiographic assessment of the right heart in adults: a report from the American Society of Echocardiography endorsed by the European Association of Echocardiography, a registered branch of the European Society of Cardiology, and the Canadian Society of Echocardiography. J Am Soc Echocardiogr. 2010 Jul;23(7):685-713; quiz 786-8.
4. Skinner JR, Stuart AG, O'Sullivan J, Heads A, Boys RJ, Hunter S. Right heart pressure determination by Doppler in infants with tricuspid regurgitation. Arch Dis Child. 1993 Aug;69(2):216-20.
5. Skinner JR, Boys RJ, Heads A, Hey EN, Hunter S. Estimation of pulmonary arterial pressure in the newborn: study of the repeatability of four Doppler echocardiographic techniques. Pediatr Cardiol. 1996 Nov-Dec;17(6):360-9.
6. Stephen B, Dalal P, Berger M, Schweitzer P, Hecht S. Noninvasive estimation of pulmonary artery diastolic pressure in patients with tricuspid regurgitation by Doppler echocardiography. Chest. 1999 Jul;116(1):73-7.
7. Lanzarini L, Fontana A, Lucca E, Campana C, Klersy C. Noninvasive estimation of both systolic and diastolic pulmonary artery pressure from Doppler analysis of tricuspid regurgitant velocity spectrum in patients with chronic heart failure. Am Heart J. 2002 Dec;144(6):1087-94.
8. Miller D, Farah MG, Liner A, Fox K, Schluchter M, Hoit BD. The relation between quantitative right ventricular ejection fraction and indices of tricuspid annular motion and myocardial performance. J Am Soc Echocardiogr. 2004 May;17(5):443-7.
9. Neilan TG, Pradhan AD, King ME, Weyman AE. Derivation of a size-independent variable for scaling of cardiac dimensions in a normal paediatric population. Eur J Echocardiogr. 2009 Jan; 10(1): 50-5.
10. George K, Sharma S, Batterham A, Whyte G, McKenna W. Allometric analysis of the association between cardiac dimensions and body size variables in 464 junior athletes. Clin Sci (Lond). 2001 Jan; 100(1):47-54.
11. Neilan TG, Pradhan AD, Weyman AE. Derivation of a size-independent variable for scaling of cardiac dimensions in a normal adult population. J Am Soc Echocardiogr. 2008 Jul; 21(7): 779-85.
12. Sahn DJ, DeMaria A, Kisslow J, Weyman A; The Committee on M-Mode Standardization of the American Society of Echocardiography. Recommendations regarding quantitation in m-mode echocardiography: results of a survey in echocardiographic measurements. Circulation 1978; 58(6): 1072-1083.
13. Lang RM, Bierig M, Devereux RB, Flachskampf FA, Foster E, Pellikka PA, Picard MH, Roman MJ, Seward J, Shanewise JS, Solomon SD, Spencer KT, Sutton MS, Stewart WJ; Chamber Quantification Writing Group; American Society of Echocardiography's

Guidelines and Standards Committee; European Association of Echocardiography. Recommendations for chamber quantification: a report from the American Society of Echocardiography's Guidelines and Standards Committee and the Chamber Quantification Writing Group, developed in conjunction with the European Association of Echocardiography, a branch of the European Society of Cardiology. J Am Soc Echocardiogr. 2005 Dec;18(12):1440-63.
14. Rudski LG, Lai WW, Afilalo J, Hua L, Handschumacher MD, Chandrasekaran K, Solomon SD, Louie EK, Schiller NB. Guidelines for the echocardiographic assessment of the right heart in adults: a report from the American Society of Echocardiography endorsed by the European Association of Echocardiography, a registered branch of the European Society of Cardiology, and the Canadian Society of Echocardiography. J Am Soc Echocardiogr. 2010 Jul;23(7):685-713.
15. Cornell CC, Kittleson MD, Della Torre P, Häggström J, Lombard CW, Pedersen HD, Vollmar A, Wey A. Allometric scaling of M-mode cardiac measurements in normal adult dogs. J Vet Intern Med. 2004 May-Jun; 18(3): 311-21.
16. Chetboul V, Tidholm A, Nicolle A, Sampedrano CC, Gouni V, Pouchelon JL, Lefebvre HP, Concordet D. Effects of animal position and number of repeated measurements on selected two-dimensional and M-mode echocardiographic variables in healthy dogs. J Am Vet Med Assoc. 2005 Sep 1;227(5):743-7.
17. Dukes-McEwan J, French A, Corcoran B. Doppler echocardiography in the dog: measurement variability and reproducibility. Veterinary Radiology & Ultrasound 2002;43:144-152.
18. Chetboul V, Sampedrano CC, Gouni V, Concordet D, Lamour T, Ginesta J, Nicolle AP, Pouchelon JL, Lefebvre HP. Quantitative assessment of regional right ventricular myocardial velocities in awake dogs by Doppler tissue imaging: repeatability, reproducibility, effect of body weight and breed, and comparison with left ventricular myocardial velocities. J Vet Intern Med. 2005 Nov-Dec;19(6):837-44.
19. Teshima K, Asano K, Iwanaga K, Koie H, Uechi M, Kato Y, Kutara K, Edamura K, Hasegawa A, Tanaka S. Evaluation of right ventricular Tei index (index of myocardial performance) in healthy dogs and dogs with tricuspid regurgitation. J Vet Med Sci. 2006 Dec;68(12):1307-13.

Echocardiographic Assessment of the Canine Right Heart:
Reference Intervals and Repeatability, Phase 3

Abstract

Objectives: Describe the repeatability of right heart echocardiographic measurements which describe pulmonary artery pressure.

Materials and Methods: 4 client-owned dogs. Dogs underwent repeated echocardiographic examination by two operators.

Results: Of the 100 within-day, between-day and between-operator coefficients of variation (CV) generated, 72 (72%) were below 20% and 46 (46%) were below 10%. Tricuspid regurgitation had the lowest CVs. The analysis of variance revealed the operator to be a significant source of variation for 16 of 20 measurements.

Conclusions: With respect to measurement repeatability, peak tricuspid regurgitation velocity is preferred for echocardiographic estimation of systolic pulmonary artery pressure. When tricuspid regurgitation is not present, the use of transpulmonic acceleration time and acceleration-to-ejection time ratio can be considered as an alternative.

Introduction

Echocardiography has been described as "an accurate, non-invasive method that can assess cardiac structure, function and bloodflow dynamics".[1] In humans, echocardiography is used to visualize the right heart, measure the dimensions and functional indices of the right heart and apply Doppler to estimate pulmonary artery pressure. In children, applying the modified Bernoulli equation to TR velocities measured by echocardiography is a valid estimate of pulmonary artery pressure.[2] Among sick neonatal children, peak TR velocities were the most repeatable estimate of pulmonary artery pressure, compared to systolic time intervals (pulmonic valve AT:ET and pre-ejection period-to-ET) and PDA ductal flow[3]. Peak TR velocity and TR velocity at the time of valve opening have also been validated as estimates of systolic and diastolic pulmonary artery pressure respectively in human adults[4,5].

In dogs, the use of tricuspid regurgitation velocities to estimate pulmonary artery pressure has not been validated with invasive pressure measurements, although it is often assumed to be valid based on the human studies. In a retrospective investigation of dogs with PH[6], peak TR velocities and PI velocities were used to identify systolic and diastolic PH respectively. This method of estimating pulmonary artery pressure has been the basis of multiple other publications[7-24].

Systolic time intervals have been examined in dogs with PH, as they have in humans. The use of systolic time intervals, which include the AT of transpulmonic flow, the ET of transpulmonic flow and the ratio of AT:ET can be useful for identifying PH in patients without TR. For example, Schober et al[15] examined healthy Boxer dogs, healthy

WHWT and WHWT with interstitial pulmonary disease (some with normal pulmonary artery pressures, some with PH and some with undetermined pulmonary artery pressure) using echocardiography. Focusing specifically on AT and AT:ET, normal values were established and cut-off values were determined that could identify the presence of PH. The reproducibility of these measurements was not determined. These findings were supported by the work of Serres et al[20], who showed a significant correlation between pulmonary artery pressure and: AT, AT:ET, the ratio of main pulmonary artery diameter to aortic diameter and the Tei index, which is the ratio of right ventricular isovolumetric contraction and relaxation time to ET.

Because echocardiography is used extensively in the diagnosis of cardiac diseases, it is potentially a useful tool to monitor response to intervention or therapy. Repeated echocardiographic measurements obtained from healthy individuals are not identical but instead, vary because of operator and instrument factors as well as inherent, biological variability in the quantity of interest. The description of measurement variation in healthy subjects, or in diseased, but clinically stable patients, defines repeatability of the test and determines the magnitude of change that reflects a "real" or clinically relevant difference in measurements. Quantification of measurement variation is therefore essential for interpretation of echocardiograms serially obtained from patients with disease; this is the case when echocardiograms are obtained from individual patients or in the context of clinical trials.

Studies of echocardiographic variability in dogs[25-27], cats[28,29] and horses[30,31] have used 4 to 8 animals, 1 to 2 echocardiographers with studies performed over the course of 3 days to 3 weeks to produce 29-96 data points. All of these studies used the coefficient

of variation to describe the reproducibility of each measurement. We attempted to evaluate the repeatability of echocardiographic measurements related to pulmonary hypertension.

Materials and Methods

Animals

This study was approved by the Institutional Animal Care and Use Committee (IACUC) of Virginia Tech. Client-owned dogs were recruited from the caseload of the veterinary teaching hospital or from those identified during a concurrent echocardiographic investigation that enrolled healthy dogs. Written, informed client consent was obtained prior to the study. Dogs were eligible for inclusion if echocardiography disclosed tricuspid valve regurgitation for which the apparent peak velocity could be defined by continuous-wave Doppler examination. Patients were included in the investigation only if they were free of clinical signs and clinically stable as determined by the patient history. Patients were considered stable if the pet-owner had not observed a change in clinical status in the two months prior to inclusion. None of the patients were receiving treatment for cardiac disease. Exclusion criteria included pulmonic stenosis and rapidly progressive disease as determined by history and physical examination. All dogs enrolled in the study were receiving heartworm preventative and/or had been shown within the last six months to be free of Dirofilaria antigenemia using a commercially available ELISA. Table 1 describes the zoographic characteristics of these dogs. Boxer dogs and dogs of presumed Boxer dog lineage were excluded because of the apparently high prevalence of ARVC in dogs of this breed.

Experimental Design

Four dogs underwent repeated echocardiographic examination by two operators, (JMG and JAA) morning and afternoon on three non-consecutive days (Monday, Wednesday and Friday of one week). Thus, each dog had 12 echocardiograms

Echocardiography

Transthoracic echocardiography was performed using an ultrasound unit[a] equipped with probes that house multi-frequency phased-array transducers. The choice of carrier frequency and variables that determine image characteristics was at the discretion of the operator and was consistent for each animal's examinations.

Each animal was gently restrained in right and then left lateral recumbency without the use of sedation. Echocardiographic images were obtained from the right and left parasternal positions. Image planes were identified and measurements were taken according to the recommendations of the ASE[32-33]. Specifically, Doppler spectrograms of right ventricular ejection, TR and, when present, PI, were recorded. For Doppler evaluation of right ventricular ejection, the pulsed-wave sample volume was placed at the tips of the open pulmonic valve. The appearance of the resulting spectrogram, as well as the audio signal, were used to optimize the Doppler signal. Doppler recordings of right ventricular ejection were recorded from both right and left parasternal transducer sites (Figures 1-2). TR was recorded from a cranial left parasternal transducer site (Figure 3) using continuous-wave Doppler; placement of the continuous-wave cursor was directed partly by the appearance of color Doppler mapping. When identified, PI was recorded by continuous-wave Doppler using left or right parasternal transducer sites.

Measurements were taken off-line from saved digital images using dedicated measurement software[b]. Measurements were averaged from a minimum of five usually consecutive heart beats. Variables obtained from Doppler spectra of right ventricular ejection time included peak velocity and selected systolic time intervals. The latter consisted of AT, defined as the time from beginning of right ventricular ejection until the time of peak velocity, and ET. The ratio AT:ET was calculated. The peak velocity of TR was recorded and the estimated right ventricular-right atrial systolic pressure gradient was derived using a simplification of the Bernoulli equation. With regard PI, the peak velocity and end-diastolic velocity were recorded. Relevant pressure gradients were derived.

Statistical Analysis

CV were generated for time within day (for each operator), day to day (also for each operator), and operator to operator variation. Fixed effects for operator, day, and time of day were assessed using mixed model ANOVA. Besides the three fixed effects, the mixed model also included dog as a random effect. For all ANOVA models, residual plots were inspected to verify model adequacy. Statistical significance was set $\alpha=0.05$. All analyses were performed using SAS version 9.2[c].

Figure 1. Right parasternal short-axis of the right ventricular outflow tract. The pulsed-wave sample volume was placed at the tips of the open pulmonic valve. Acceleration time was measured from the onset to the peak of flow. Ejection time was measured from the onset to the end of transpulmonic flow. Peak transpulmonic flow was measured, as was peak and end-diastolic pulmonic insufficiency, if present.

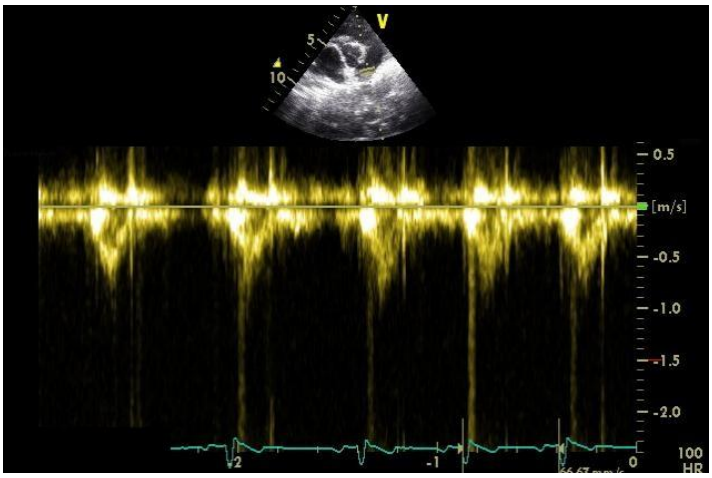

Figure 2. Left parasternal short-axis of the right ventricular outflow tract. The pulsed-wave sample volume was placed at the tips of the open pulmonic valve. Acceleration time was measured from the onset to the peak of flow. Ejection time was measured from the onset to the end of transpulmonic flow. Peak transpulmonic flow was measured, as was peak and end-diastolic pulmonic insufficiency, if present.

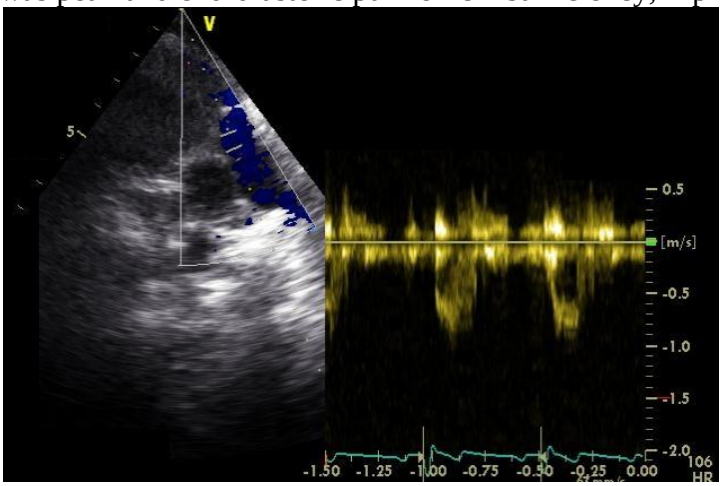

Figure 3. Left parasternal four-chamber view of the right ventricle, optimized for right ventricular inflow. Peak tricuspid regurgitation velocity was measured using continuous wave Doppler.

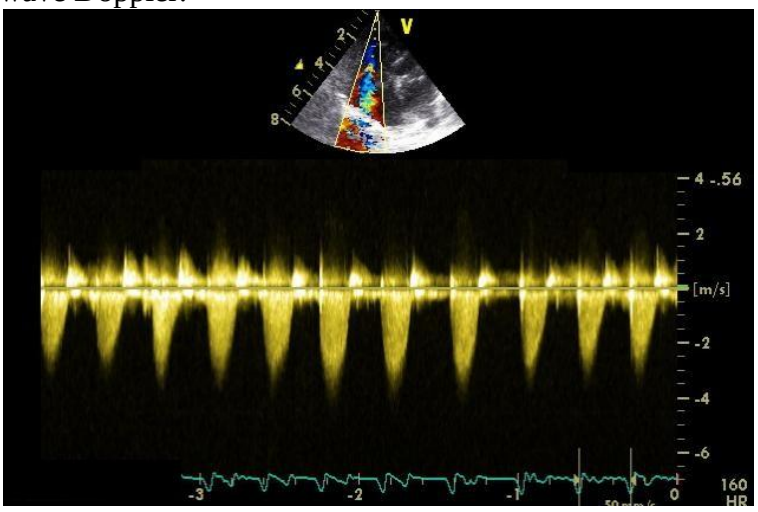

[a] Vivid 7 Dimension, GE Healthcare, Waukesha WI

[b] EchoPAC dimension v.6.1.x, GE Healthcare Technologies, Milwaukee, WI, USA

[c] SAS, version 9.2, Carey NC, USA

Results

Four client-owned dogs were recruited; their characteristics are summarized in Table 1. The within-day, between-day and between-user coefficients of variation are summarized in Table 2a. Of the 100 CV generated, 46 were less than 10% and 64 were below 15%. Of the 54 CV that were greater than 10%, 15 belonged to operator 1 (9 within-day and 6 between-day) and 24 belonged to operator 2 (12 within-day and 12 between-day). Tricuspid regurgitation had the lowest CVs. The significant fixed effects of operator, day or time of day are listed in Table 2b. The analysis of variance revealed the operator to be a significant source of variation for 16 of 20 measurements.

Table 1: Zoographic characteristics of the dogs with tricuspid regurgitation

Characteristic	Dogs
Age (years)	8.3 ± 5.1
Sex Female Male	 Spayed (3), Intact (0) Neutered (1), Intact (0)
Body weight (kg)	33.4 ± 24.2
Body surface area (cm^3)	0.60 ± 0.3
Breed	Mixed breed (1) Labrador retriever (1) Dachshund (1) Australian shepherd (1)
Concurrent cardiac diseases	Myxomatous mitral and tricuspid valve disease (3) Tricuspid valve dysplasia (1)

Table 2a. Coefficients of variation, with values greater than 10% in bold.

	Operator 1	Operator 2	Operator 1	Operator 2	CV between-operator (%)
	CV within-day (%)		CV between-day(%)		
2D right parasternal short axis					
Peak velocity of right ventricular ejection (PV_Vmax_R)	6.9	**10.1**	5.2	7.0	8.1
Peak pressure gradient of right ventricular ejection (PV_maxPG_R)	**13.6**	**20.0**	**10.5**	**14.1**	**16.2**
Trans-pulmonic acceleration time (PV_AT_R)	**12.2**	9.8	5.7	8.4	**27.8**
Trans-pulmonic ejection time (PV_ET_R)	5.1	7.3	5.4	5.9	8.8
Acceleration-to-ejection time ratio (AT_ET_ratio_R)	9.7	9.1	8.0	**11.4**	**17.9**
Peak velocity of pulmonic valve insufficiency (PI_Vmax_R)	**13.6**	**28.8**	7.2	**21.0**	8.7
Peak pressure gradient of pulmonic valve insufficiency (PI_maxPG_R)	**26.4**	**53.0**	**13.9**	**41.3**	**16.4**
Velocity of end-diastolic pulmonic insufficiency (endPI_Vmax_R)	4.0	**32.3**	2.2	**34.1**	**42.0**
Peak pressure gradient of end-diastolic pulmonic insufficiency (endPI_PG_R)	8.2	**60.0**	4.0	**66.6**	**69.6**
2D left parasternal short axis					
Peak velocity of right ventricular ejection (PV_Vmax_L)	6.1	4.7	7.0	6.7	**11.0**
Peak pressure gradient of right ventricular ejection (PV_maxPG_L)	**12.4**	8.9	**14.0**	**13.7**	**21.8**
Trans-pulmonic acceleration time (PV_AT_L)	7.7	**12.1**	7.2	6.3	**30.6**
Trans-pulmonic ejection time (PV_ET_L)	5.3	4.5	4.2	6.5	6.9
Acceleration-to-ejection time ratio (AT_ET_ratio_L)	9.4	**11.9**	7.6	7.9	**26.8**
Peak velocity of pulmonic valve insufficiency (PI_Vmax_L)	**13.8**	**18.0**	7.8	**11.2**	**34.4**
Peak pressure gradient of pulmonic valve insufficiency (PI_maxPG_L)	**26.4**	**33.5**	**14.4**	**21.2**	**60.4**
Velocity of end-diastolic pulmonic insufficiency (endPI_Vmax_L)	**17.1**	**26.4**	**12.9**	**42.5**	**58.8**
Peak pressure gradient of end-diastolic pulmonic insufficiency (endPI_PG_L)	**32.8**	**46.4**	**24.2**	**76.3**	**96.4**
2D left parasternal four-chamber					
Peak velocity of tricuspid regurgitation (TR_Vmax_L)	3.2	7.2	3.7	5.4	7.1
Peak pressure gradient of tricuspid regurgitation (TR_maxPG_L)	6.4	14.2	7.5	**10.7**	**14.0**

Table 2b. Significant ANOVA fixed effects

	Significant ANOVA Fixed effect
2D right parasternal short axis	
Peak velocity of right ventricular ejection (PV_Vmax_R)	Operator
Peak pressure gradient of right ventricular ejection (PV_maxPG_R)	Operator
Trans-pulmonic acceleration time (PV_AT_R)	Operator
Trans-pulmonic ejection time (PV_ET_R)	Operator, time of day
Acceleration-to-ejection time ratio (AT_ET_ratio_R)	Operator, day
Peak velocity of pulmonic valve insufficiency (PI_Vmax_R)	Operator
Peak pressure gradient of pulmonic valve insufficiency (PI_maxPG_R)	Operator, time of day
Velocity of end-diastolic pulmonic insufficiency (endPI_Vmax_R)	Operator, day
Peak pressure gradient of end-diastolic pulmonic insufficiency (endPI_PG_R)	Operator
2D left parasternal short axis	
Peak velocity of right ventricular ejection (PV_Vmax_L)	-
Peak pressure gradient of right ventricular ejection (PV_maxPG_L)	-
Trans-pulmonic acceleration time (PV_AT_L)	Operator
Trans-pulmonic ejection time (PV_ET_L)	Operator
Acceleration-to-ejection time ratio (AT_ET_ratio_L)	Operator
Peak velocity of pulmonic valve insufficiency (PI_Vmax_L)	Operator
Peak pressure gradient of pulmonic valve insufficiency (PI_maxPG_L)	Operator
Velocity of end-diastolic pulmonic insufficiency (endPI_Vmax_L)	Operator, day
Peak pressure gradient of end-diastolic pulmonic insufficiency (endPI_PG_L)	Operator, day
2D left parasternal four-chamber	
Peak velocity of tricuspid regurgitation (TR_Vmax_L)	-
Peak pressure gradient of tricuspid regurgitation (TR_maxPG_L)	-

Discussion

In studies of human echocardiography, the repeatability of tricuspid regurgitation velocity is typically high. This has been documented in pediatric[34] and adult[35] populations and in cases of physiologic tricuspid regurgitation[36]. Similarly, the peak velocity of TR was the measurement with the lowest coefficients of variation in our dogs.

The use of both right and left parasternal transducer sites to obtain systolic time intervals is associated with low CV. Schober, et al[37] established AT and the AT:ET as significant predictors of pulmonary hypertension. In this study, AT and AT:ET were associated with within-day and between-day CVs of less than 12.2%, but between-operator CVs of 17.9-27.8%. This study provides reinforces the usefulness of AT and AT:ET by confirming that the variability of the measurement is low, however the study may also suggest that a single echocardiographer should evaluate a patient serially.

From these findings, measurement of TR velocity should be the first priority in the echocardiographic estimation of systolic pulmonary artery pressure. If TR is not present, we recommend the use of AT and AT:ET to indirectly assess pulmonary artery pressure. Similarly, the ASE Guidelines for the Echocardiographic Assessment of the Right Heart in Adults[33] recommends measuring TR velocity in all patients with TR and assessing diastolic pulmonary artery pressure in patients with PH or heart failure. This report does not comment on the usefulness of other validated methods of assessing pulmonary hemodynamics but references a State of the Art review[38] which recommends direct or indirect estimation of pulmonary artery pressure in every echocardiogram. This review describes a hierarchy of preferred measurements to assess pulmonary artery

pressure: the preferred measurement is velocity of TR. In the absence of TR, diastolic pulmonary pressure should be assessed using PI velocity. If neither of these velocity measurements is possible, the pulmonary artery pressure should be indirectly assessed using PV AT or Doppler tissue imaging-derived right ventricular regional isovolumic relaxation time (Doppler tissue imaging was not employed in this study). The findings of this study align with the recommendations of ASE where it concerns the use of TR velocity and PV AT. Our findings differed in that we recommend the use of the AT:ET ratio and do not advocate the use of PI velocity because of its high variability.

Concerning variability, of the 100 within-day, between-day and between-operator CVs generated by this study, 54 were greater than 10% and 28 were greater than 20%. Experience may play a role in this, since Operator 2 tended to have higher CVs than Operator 1. Additionally, many of the variables were calculated pressure gradients, which are generated using the modified Bernoulli equation in which the measured velocity is taken to the second exponent. Following, the variability of the PG measurements would be compounded so higher CVs are expected for these values. Finally the hemodynamics of the right heart are affected by the respiratory cycle[39,40]. Decreased intrathoracic pressure during inspiration increases blood flow into and through the right heart. Because of ventricular interdependence, left ventricular flow is reduced during inspiration but increases during expiration, when blood flow through the right heart is reduced. To counteract the effects of the respiratory cycle somewhat, measurements were taken from a minimum of five consecutive heart beats and then averaged.

This study's limitations include the small number of subjects with different underlying causes of TR. The study protocol provided 48 data points for each echocardiographic measurement. This number is consistent with the design of previous studies of echocardiographic variability in dogs, cats and horses which produced 29-96 data points for each echocardiographic measurement. Further investigation could be targeted at recruiting larger, more homogenous study populations. In addition, further studies involving clinical patients with elevated pulmonary artery pressure are warranted.

References

1. Moïse NS and Fox PR. Echocardiography and Doppler Imaging. In Fox PR, Sisson DD, and Moïse NS (eds). Textbook of Canine and Feline Cardiology: Principles and Clinical Practice, 2nd ed. Saunders: Philadelphia 1999. 130-171.
2. Skinner JR, Stuart AG, O'Sullivan J, Heads A, Boys RJ, Hunter S. Right heart pressure determination by Doppler in infants with tricuspid regurgitation. Arch Dis Child. 1993 Aug;69(2):216-20.
3. Skinner JR, Boys RJ, Heads A, Hey EN, Hunter S. Estimation of pulmonary arterial pressure in the newborn: study of the repeatability of four Doppler echocardiographic techniques. Pediatr Cardiol. 1996 Nov-Dec;17(6):360-9.
4. Stephen B, Dalal P, Berger M, Schweitzer P, Hecht S. Noninvasive estimation of pulmonary artery diastolic pressure in patients with tricuspid regurgitation by Doppler echocardiography. Chest. 1999 Jul;116(1):73-7.
5. Lanzarini L, Fontana A, Lucca E, Campana C, Klersy C. Noninvasive estimation of both systolic and diastolic pulmonary artery pressure from Doppler analysis of tricuspid regurgitant velocity spectrum in patients with chronic heart failure. Am Heart J. 2002 Dec;144(6):1087-94.
6. Johnson L, Boon J, Orton EC. Clinical characteristics of 53 dogs with Doppler-derived evidence of pulmonary hypertension: 1992-1996. J Vet Intern Med. 1999 Sep-Oct;13(5):440-7.
7. Corcoran BM, Cobb M, Martin MW, Dukes-McEwan J, French A, Fuentes VL, Boswood A, Rhind S. Chronic pulmonary disease in West Highland white terriers. Vet Rec. 1999 May 29;144(22):611-6.
8. Bertazzolo W, Zuliani D, Pogliani E, Caniatti M, Bussadori C. Diffuse bronchiolo-alveolar carcinoma in a dog. J Small Anim Pract. 2002 Jun;43(6):265-8.
9. Webb JA, Armstrong J. Chronic idiopathic pulmonary fibrosis in a West Highland white terrier. Can Vet J. 2002 Sep;43(9):703-5.
10. Glaus TM, Soldati G, Maurer R, Ehrensperger F. Clinical and pathological characterisation of primary pulmonary hypertension in a dog. Vet Rec. 2004 Jun 19;154(25):786-9.
11. Kolm US, Amberger CN, Boujon CE, Lombard CW. Plexogenic pulmonary arteriopathy in a Pembroke Welsh corgi. J Small Anim Pract. 2004 Sep;45(9):461-6.
12. Norris AJ, Naydan DK, Wilson DW. Interstitial lung disease in West Highland White Terriers. Vet Pathol. 2005 Jan;42(1):35-41.
13. Bach JF, Rozanski EA, MacGregor J, Betkowski JM, Rush JE. Retrospective evaluation of sildenafil citrate as a therapy for pulmonary hypertension in dogs. J Vet Intern Med. 2006; 20: 1132-1135.
14. Nicolle AP, Chetboul V, Tessier-Vetzel D, Carlos Sampedrano C, Aletti E, Pouchelon JL. Severe pulmonary arterial hypertension due to Angiostrongylosus vasorum in a dog. Can Vet J. 2006 Aug;47(8):792-5.
15. Schober KE, Baade H. Doppler echocardiographic prediction of pulmonary hypertension in West Highland white terriers with chronic pulmonary disease. J Vet Intern Med. 2006 Jul-Aug;20(4):912-20.
16. Serres F, Nicolle AP, Tissier R, Gouni V, Pouchelon JL, Chetboul V. Efficacy of oral tadalafil, a new long-acting phosphodiesterase-5 inhibitor, for the short-term treatment of

pulmonary arterial hypertension in a dog. J Vet Med A Physiol Pathol Clin Med. 2006 Apr; 53(3): 129-133.
17. Serres FJ, Chetboul V, Tissier R, Carlos Sampedrano C, Gouni V, Nicolle AP, Pouchelon JL. Doppler echocardiography-derived evidence of pulmonary arterial hypertension in dogs with degenerative mitral valve disease: 86 cases (2001-2005). J Am Vet Med Assoc. 2006 Dec 1;229(11):1772-8.
18 Zabka TS, Campbell FE, Wilson DW. Pulmonary arteriopathy and idiopathic pulmonary arterial hypertension in six dogs. Vet Pathol. 2006 Jul;43(4):510-22.
19. Paige CF, Abbott JA, Pyle RL. Systolic anterior motion of the mitral valve associated with right ventricular systolic hypertension in 9 dogs. J Vet Cardiol. 2007 (9): 9-14.
20. Serres F, Chetboul V, Gouni V, Tissier R, Sampedrano CC, Pouchelon JL. Diagnostic value of echo-Doppler and tissue Doppler imaging in dogs with pulmonary arterial hypertension. J Vet Intern Med. 2007 Nov-Dec;21(6):1280-9.
21. Russell NJ, Irwin PJ, Hopper BJ, Olivry T, Nicholls PK. Acute necrotizing pulmonary vasculitis and pulmonary hypertension in a juvenile dog. J Small Anim Pract. 2008 Jul;49(7):349-55.
22. Chiavegato D, Borgarelli M, D'Agnolo G, Santilli RA. Pulmonary hypertension in dogs with mitral regurgitation attributable to myxomatous valve disease. Vet Radiol Ultrasound. 2009 May-Jun;50(3):253-8.
23. Seibert RL, Maisenbacher HW 3rd, Prosek R, Adin DB, Arsenault WG, Estrada AH. Successful closure of left-to-right patent ductus arteriosus in three dogs with concurrent pulmonary hypertension. J Vet Cardiol. 2010 Apr; 12(1): 67-73.
24. Heikkilä HP, Lappalainen AK, Day MJ, Clercx C, Rajamäki MM. Clinical, Bronchoscopic, Histopathologic, Diagnostic Imaging, and Arterial Oxygenation Findings in West Highland White Terriers with Idiopathic Pulmonary Fibrosis. J Vet Intern Med. 2011 Mar 2.
25. Dukes-McEwan J, French AT, Corcoran BM. Doppler echocardiography in the dog: measurement variability and reproducibility. Vet Radiol Ultrasound. 2002 Mar-Apr;43(2):144-52.
26. Chetboul V, Athanassiadis N, Carlos C, Nicolle A, Zilberstein L, Pouchelon JL, Lefebvre HP, Concordet D. Assessment of repeatability, reproducibility, and effect of anesthesia on determination of radial and longitudinal left ventricular velocities via tissue Doppler imaging in dogs. Am J Vet Res. 2004 Jul;65(7):909-15.
27. Chetboul V, Tidholm A, Nicolle A, Sampedrano CC, Gouni V, Pouchelon JL, Lefebvre HP, Concordet D. Effects of animal position and number of repeated measurements on selected two-dimensional and M-mode echocardiographic variables in healthy dogs. J Am Vet Med Assoc. 2005 Sep 1;227(5):743-7.
28. Chetboul V, Concordet D, Pouchelon JL, Athanassiadis N, Muller C, Benigni L, Munari AC, Lefebvre HP. Effects of inter- and intra-observer variability on echocardiographic measurements in awake cats. J Vet Med A Physiol Pathol Clin Med. 2003 Aug;50(6):326-31.
29. Simpson KE, Devine BC, Gunn-Moore DA, French AT, Dukes-McEwan J, Koffas H, Moran CM, Corcoran BM. Assessment of the repeatability of feline echocardiography using conventional echocardiography and spectral pulse-wave Doppler tissue imaging techniques. Vet Radiol Ultrasound. 2007 Jan-Feb;48(1):58-68.

30. Schwarzwald CC, Schober KE, Bonagura JD. Methods and reliability of echocardiographic assessment of left atrial size and mechanical function in horses. Am J Vet Res. 2007 Jul;68(7):735-47.
31. Buhl R, Ersbøll AK, Eriksen L, Koch J. Sources and magnitude of variation of echocardiographic measurements in normal standardbred horses. Vet Radiol Ultrasound. 2004 Nov-Dec;45(6):505-12.
32. Lang RM, Bierig M, Devereux RB, Flachskampf FA, Foster E, Pellikka PA, Picard MH, Roman MJ, Seward J, Shanewise JS, Solomon SD, Spencer KT, Sutton MS, Stewart WJ; Chamber Quantification Writing Group; American Society of Echocardiography's Guidelines and Standards Committee; European Association of Echocardiography. Recommendations for chamber quantification: a report from the American Society of Echocardiography's Guidelines and Standards Committee and the Chamber Quantification Writing Group, developed in conjunction with the European Association of Echocardiography, a branch of the European Society of Cardiology. J Am Soc Echocardiogr. 2005 Dec;18(12):1440-63.
33. Rudski LG, Lai WW, Afilalo J, Hua L, Handschumacher MD, Chandrasekaran K, Solomon SD, Louie EK, Schiller NB. Guidelines for the echocardiographic assessment of the right heart in adults: a report from the American Society of Echocardiography endorsed by the European Association of Echocardiography, a registered branch of the European Society of Cardiology, and the Canadian Society of Echocardiography. J Am Soc Echocardiogr. 2010 Jul;23(7):685-713.
34. Skinner JR, Boys RJ, Heads A, Hey EN, Hunter S. Estimation of pulmonary arterial pressure in the newborn: study of the repeatability of four Doppler echocardiographic techniques. Pediatr Cardiol. 1996 Nov-Dec;17(6):360-9.
35. Stephen B, Dalal P, Berger M, Schweitzer P, Hecht S. Noninvasive estimation of pulmonary artery diastolic pressure in patients with tricuspid regurgitation by Doppler echocardiography. Chest. 1999 Jul;116(1):73-7.
36. Lavie CJ, Hebert K, Cassidy M. Prevalence and severity of Doppler-detected valvular regurgitation and estimation of right-sided cardiac pressures in patients with normal two-dimensional echocardiograms. Chest. 1993 Jan;103(1):226-31
37. Schober KE, Baade H. Doppler echocardiographic prediction of pulmonary hypertension in West Highland white terriers with chronic pulmonary disease. J Vet Intern Med. 2006 Jul-Aug;20(4):912-20.
38. Milan A, Magnino C, Veglio F. Echocardiographic indexes for the non-invasive evaluation of pulmonary hemodynamics. J Am Soc Echocardiogr. 2010 Mar;23(3):225-39
39. Feihl F, Broccard AF. Interactions between respiration and systemic hemodynamics. Part I: basic concepts. Intensive Care Med. 2009 Jan;35(1):45-54.
40. Feihl F, Broccard AF. Interactions between respiration and systemic hemodynamics. Part II: practical implications in critical care. Intensive Care Med. 2009 Feb;35(2):198-205.

Conclusions

This study is the first to define standard imaging planes for echocardiographic assessment of the canine right heart. The imaging planes and measurements were similar to those proposed by the ASE in 2010 and used in human cardiology. With adequate understanding of the planes, the images were not difficult to obtain and could be easily adopted by trained veterinary echocardiographers. The ultimate goal of this study was the determination of the echo-derived measurement means, prediction intervals and repeatability estimates which could be applied to clinical cases and clinical research related to diseases of the right heart.

The repeatability arm of the first study described the least and most repeatable approaches to echocardiographic evaluation of the right heart. Values for the CVs ranged from 1.5% to 86.2% with 195 of the 210 calculated CVs below 20%. Most of the CVs over 20% "between operator" variation, indicating that comparison studies are ideally performed and measured by the same operator.

In studies of human echocardiography, the repeatability of TR velocity is typically high. Similarly, the peak velocity of TR was the measurement with the lowest coefficients of variation in the second study. The second study also revealed the use of both right and left parasternal transducer sites to obtain systolic time intervals is associated with low CV. In this study, AT and AT:ET were associated with within-day and between-day CVs of less than 12.2%, but between-operator CVs of 17.9-27.8%. This study reinforces the usefulness of AT and AT:ET by confirming that the variability

of the measurement is low, however the study may also suggest that a single echocardiographer should evaluate a patient serially.

Based on the findings of our study we recommend imaging the right atrium from either the right parasternal long axis or left parasternal four-chamber views. The right ventricle is best imaged from the left parasternal four-chamber plane. The caudal vena cava can also be assessed from a modified four-chamber view. The left parasternal short axis provides repeatable measurement of the right ventricular outflow tract and main pulmonary artery. The pulmonic valve and aortic valve dimensions and ratio were repeatable in the right parasternal short axis view. Measurement of the TR velocity should be the first priority in echocardiographic estimation of systolic pulmonary artery pressure. If tricuspid regurgitation is not present, we recommend the use of AT and AT:ET to indirectly assess pulmonary artery pressure. Interestingly, our recommendations are similar to those put forth by the ASE in their guidelines for the echocardiographic evaluation of the right heart.